AD NUMBER

AD864185

NEW LIMITATION CHANGE

TO

Approved for public release, distribution unlimited

FROM

Distribution authorized to U.S. Gov't. agencies and their contractors; Critical Technology; 12 JAN 1970. Other requests shall be referred to Air Force Rocket Propulsion Lab., Edwards AFB, CA.

AUTHORITY

AFRPL ltr, 29 Sep 1971

AFRPL-TR-69-247

ELECTROLYTIC IGNITION SYSTEM FOR MONOPROPELLANTS

FINAL REPORT
(CONTRACT F04611-69-C-0048)

JANUARY 1970

by

B. P. Breen, M. Gerstein, M. A. McLain

DYNAMIC SCIENCE
A Division of Marshall Industries
2400 Michelson Drive, Irvine, California

AIR FORCE ROCKET PROPULSION LABORATORY
DIRECTORATE OF LABORATORIES
AIR FORCE SYSTEMS COMMAND
UNITED STATES AIR FORCE
EDWARDS, CALIFORNIA

SPECIAL NOTICE

When U.S. Government drawings, specifications, or other data are used for any purpose other than a definitely related Government procurement operation, the Government thereby incurs no responsibility nor any obligation whatsoever, and the fact that the Government may have formulated, furnished, or in any way supplied the said drawings, specifications, or other data, is not to be regarded by implication or otherwise, or in any manner licensing the holder or any other person or corporation, or conveying any rights or permission to manufacture, use, or sell any patented invention that may in any way be related thereto.

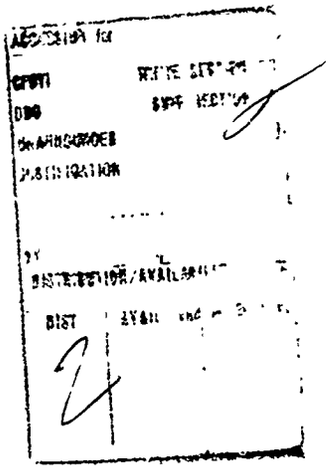

AFRPL-TR-69-247

ELECTROLYTIC IGNITION SYSTEM FOR MONOPROPELLANTS

Contract F04611-69-C-0048

12 January 1970

By: B. P. Breen, M. Gerstein and M.A.McLain
DYNAMIC SCIENCE, a Division of Marshall Industries
2400 Michelson Drive, Irvine, California 92664

For:
AIR FORCE ROCKET PROPULSION LABORATORY
Directorate of Laboratories
Air Force Systems Command
United States Air Force
Edwards, California 93523

FOREWORD

The research documented in this final report was sponsored by the Air Force Rocket Propulsion Laboratory, Edwards, California, under Contract F04611-69-C-0048. The program was conducted by the Dynamic Science Division of Marshall Industries under the direction of Lt. Douglas D. Huxtable, USAF/RPCL. The period covered under this contract was 3 February 1969 to 31 July 1969.

The Dynamic Science Program Manager was Dr. B. P. Breen. The laboratory test program was run by Miss M. A. McLain. Both Dr. Breen and Miss McLain were advised and assisted by Dr. Melvin Gerstein.

This technical report has been reviewed and is approved.

W. H. Ebelke, Colonel, USAF
Chief, Propellant Division

SUMMARY

It was the objective of this work to utilize the electrolytic decomposition of hydrazine toward the improvement of starting pressurization transients in monopropellant rockets. The electrochemistry and heat generation involved during the electrolytic decomposition of propellant grade hydrazine was examined by means of polarography and chromatographic examination of the decomposition gases. Critical voltages of decomposition and related data obtained were incorporated into a thermal ignition model to aid in the design of a flow system ignition cell.

It was found that engine ignition times of 2 to 5 milliseconds and pulse start transients of less than 15 milliseconds could be obtained in a simulated one-half thrust configuration. The ignition data and chamber pressure traces included in this report demonstrate the reproducibility of electrolytic ignitions through the electrolytic decomposition of hydrazine. Although the primary concern of this work was engine start-up, variables necessary to optimize ignition delay and maintain sustained engine operation after start-up were investigated. Total optimization of the system was beyond the scope of this present effort.

TABLE OF CONTENTS

LIST OF FIGURES

LIST OF FIGURES (Continued)

SECTION I
INTRODUCTION

1.0 OBJECTIVE

The principle objective of this work was to demonstrate the application of electrolytic decomposition of hydrazine to improve starting pressurization transients of monopropellant rocket engines. Necessary experimental and analytical studies were performed concerning electrolysis energy requirements and decomposition heat release mechanisms. These studies established both the feasibility of using electrolysis to ignite a hydrazine based monopropellant and the parameters necessary in the initial design of a practical engine ignition system.

Dynamic Science has applied electrolysis techniques to demonstrate the unique concept that ignition can be accomplished by means of heat liberated by the electrolytic decomposition of an exothermic monopropellant. It was demonstrated that ignition times with the hydrazine monopropellant system could be as short as five milliseconds, and that thermal configurations could be designed to sustain decomposition.

Demonstration of this concept has continued with this research which has as its purpose the fully instrumented definition of chamber pressure start transients. In the following discussion oscillograph traces of engine ignition times of 2 to 5 millieseconds and pulse start transients of less than 15 ms are shown to have been obtained.

2.0 MONOPROPELLANT IGNITION SYSTEMS

The use of monopropellant engines for attitude control systems is extremely desirable due to the system reliability (one valve and tankage as opposed to two delivery and control systems) and the ability to reproduce impulse bits without hard starts. Various schemes are being used or are proposed to ignite the propellant; among these are catalyst surfaces, heat (electrical resistance heating), oxidizer slugs, and the electrolysis concept presented here.

Reactions on catalytic surfaces have been the primary means of achieving ignition with monopropellants. Hydrogen peroxide reactions on silver catalysts and hydrazine reaction on Shell 405 catalysts are the most commonly used combinations. However, initial starting transients are longer than desirable and vary as the bed temperature rises. Also, catalytic surfaces apparently do not exist for all of the commonly used methylated hydrazine fuels and fuel/additive blends. Problems associated with the use of catalysts are: carbon contamination when used with methylated hydrazine and hydrazine blends, possible loss of reactivity during space storage, damage from thermal transients, and irreproducible pulses due to the temperature of the catalyst. Ablative chambers cannot be used with catalysts due to possible contamination of the catalysts.

Hydrazine based fuels can also be decomposed by heat (Refs. 1, 2, and 3) (resistojet type thrustor). However, for pulse mode operation, the programming of a heat source ahead of the fuel flow can be difficult because the thermal lag depends upon temperature history. The main advantage of the Hydrazine Electrolysis Injector over the resistojet type thrustor is that electrolysis can contribute the heat of decomposition at the ambient temperature, thereby allowing reproducible trains of pulses without a warmup period for the hardware.

Electrolytic decomposition of hydrazine appears to offer many advantages over the above mentioned systems. For example, in electrolytic decomposition there is no contamination problem, no preignition heating cycle, simplicity of operation, and potentially ignition within reproducible time periods shorter than those possible with catalytic beds. For specific missions an electrolytic engine might have many advantages over currently used engines while the use of an Electrolysis Injector in conjunction with current beds would substantially improve their initial pulse train, impulse per pulse and pulse centroid.

The electrolysis of inorganic molecules in liquid solutions is a standardized and useful analytical and electrochemical technique. Thus the electrolytic decomposition of hydrazine would appear to be an obvious method of generating gaseous products and a large quantity of heat. In most electrolysis applications, the enthalpy of formation or decomposition is considered a liability to the process and provisions must be made for process cooling (such as when charging a battery or operating a plating bath). However, it is this heat of decomposition which can be used as the ignition source in a properly designed transient start engine system.

A gas generator currently being developed by Hughes (Ref. 4) under Contract 951720 of Jet Propulsion Laboratory is a good example of both the feasibility of electrolyzing hydrazine and the difficulty of heat removal. In this concept the hydrazine is electrolyzed directly in the tank and the gaseous decomposition products are used for tank pressurization and to create sufficient gases for cold gas thrusters. However, if a great deal of gas is needed the tankage system may overheat with disastrous effects. Thus this application is a good example where the heat release due to electrolytic decomposition is a liability. It also demonstrates that, rather than lose the chemical energy of decomposition as waste heat, this heat can be used as an ignition source.

Most important, this work (Ref. 4) under the technical direction of Mr. A. Karbin and Mr. David D. Evans of the Jet Propulsion Laboratory, demonstrates the feasibility of electrolyzing hydrazine. It is the unique concept of Dynamic Science that this electrolysis be used to liberate the heat of decomposition so as to generate an ignition source.

Thus, in an independent application of this concept to monopropellant ignition, Dynamic Science has built several small thrustors, such as shown in Figures 22, 23, 25, and 27 of Section II of this report. Although these thrustors were simple in design they were capable of ambient temperature starts of the order of microseconds. Thus the concept of electrolytic monopropellant starts does work. Because of previous experience with electrochemistry, the Hughes cold gas generator (Ref. 4) and Dynamic Science's Engine Start Program, we feel that the Electrolysis Injector concept will prove highly successful in producing essentially instantaneous starts.

3.0 ELECTROCHEMICAL PROPERTIES OF HYDRAZINE AND APPLICATIONS IN A NONFLOW SYSTEM

The first phase of this program was initiated in an attempt to understand the electrochemistry and heat generation involved during the electrolytic decomposition of propellant grade hydrazine. Current/voltage measurements were made in order to determine specific conductivity and off-gases were analyzed for various voltages and electrode materials and it was found that the predominant gases, as was expected, were N_2, H_2, and NH_3. Copper and silver electrodes

provided a greater volume of off gases than did the stainless steel or the platinum electrodes when operating under equal conditions. However, too much precipitate was formed using copper or silver to make them practical for use as electrodes in an ignition system. Polarograph studies were conducted in order to define decomposition voltages for hydrazine and MMH. This analysis afforded the necessary guidelines for the design and testing of typical stagnation cells by providing critical voltage data used to define a thermal ignition model with electrolytic decomposition. Factors affecting electrolysis ignition were established in the areas of electrical factors, fundamentals of electrolytic conduction and optimization of geometry through extensive testing of electrolytic ignition in the stagnation system.

4.0 ELECTROLYTIC IGNITION OF HYDRAZINE IN A FLOW SYSTEM

In the second phase of the program emphasis was directed toward the design, construction, and operation of a nominal 1/2 thrust electrolytic ignition injector device. Several flow systems were designed and tested. Design variations in the flow system consisted of different electrode configurations and areas, varied materials used in the basic hardware and changes in the diameter of the exhaust nozzle orifice. Problems encountered during the operation of the various flow systems involved poor control of vapor generation and electrode insulation. The first difficulty resulted in an inability to maintain steady state operation after ignition and the second caused frequent shorting of the cell. However, many electrolytic starts were made in as short a time as 4 milliseconds and chamber pressures as great as 90 psi were recorded. In several instances chamber pressures greatly exceeding 90 psi occurred and the test cells exploded. Detailed discussion of the work described in Section I, Items 3 and 4 follows in Section II of this report.

SECTION II

ELECTROLYSIS STUDIES OF HYDRAZINE AND MONOMETHYLHYDRAZINE

1.0 INTRODUCTION

The technique of starting a monopropellant hydrazine rocket engine by means of electrolysis involves the electrolytic decomposition of a monopropellant by low level voltage. Such decomposition results in a large amount of heat generation due to the propellants heat of decomposition. When the rate of heat generation is properly matched to low hardware heat diffusivity, a rapid temperature rise transient leads to subsequent stable thermal ignition.

Maximum heat generation from decomposition is desirable for the electrolytic ignition of hydrazine propellants, and such maximum heat is involved when hydrazine decomposes according to the formula:

$$N_2H_4^{(\ell)} \rightarrow 4/3\ NH_3^{(g)} + 1/3\ N_2^{(g)} \qquad (1)$$

Preliminary studies were aimed at defining the basic conductivity, off-gas electrolysis and critical voltages involved when approaching the breakdown described by Formula #1 during the electrolytic decomposition of hydrazine.

2.0 OFF-GAS DUE TO ELECTROLYTIC DECOMPOSITION OF HYDRAZINE

a. Apparatus

Electrolysis runs were made using a standard U-tube electrolysis unit (closely resembling a Hoffman unit) modified to facilitate gas sampling as shown in Figure 1. DC power was supplied by two standard automobile batteries connected in series and tapped to provide 15 volts. A DC voltmeter and DC milliammeter were placed in the circuit. Interchangeable electrodes were made using 0.062 inch diameter, 302 stainless steel, 0.062 diameter copper wire, 99% pure platinum wire, .025 inch diameter, and 99% pure silver wire, 0.062 inch diameter. A Barber Colman chromatograph equipped with a Carle thermoconductivity microcell was used for the analyses of the gases evolved during electrolytic decomposition of the hydrazine blends. An 8 ft long, 1/4 in. diameter column of molecular sieve 5A 40/50 mesh was used to determine N_2 and H_2 and a Porapak Q column 6 ft. long, 1/4 inch diameter was used for the detection of NH_4. The conditions of analyses were carried out using these conditions: Carrier Gas - Helium; Flowrate - 40 cc/min; Column Temperature - 70°C.

b. Procedure

A 2.0% ammonium nitrate addition was chosen as the electrolyte and 15 volt DC as constant voltage because in previous runs using stainless steel electrodes these conditions somewhat represented a middle area of

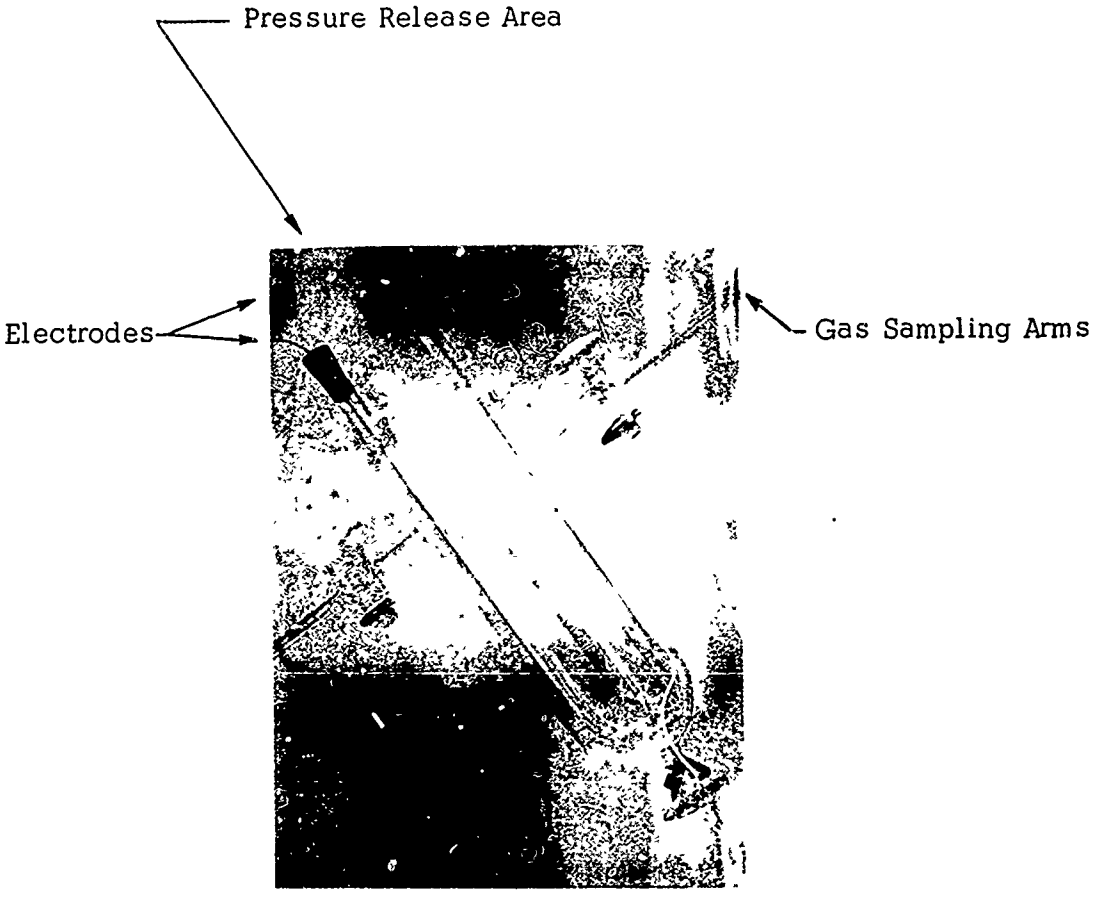

Figure 1. Hoffman Electrolysis Apparatus with Side Arm Modification.

electrolytic activity, and afforded greater control during the sampling of the decomposition gases. One run each was made, using .062 in. dia., 302 SS, .062 in. dia. copper, .025 in. dia. copper, .025 in. dia. 99% pure platinum, and .062 in. dia. 99% pure silver wire. The electrodes were 2-1/2 in. apart and were immersed six inches into the electrolyte. This combination gave a current flow of approximately 4 milliamps with all materials. No provisions were made for monitoring the temperature of these runs but attempts were made to collect and analyze the gases of decomposition. Runs were held to two hours each and a comparison of the amount of decomposition of each run was made by measuring the cc's of gas evolved at each electrode for a given run.

c. Discussion of Results

Decomposition Gas Composition

The decomposition gases on all runs were collected in evacuated tubes and attempts were made to analyze the samples by means of gas chromatography. Table 1 indicates the cc's of decomposition gases evolved, and those gases identifiable for each run; other gases appeared to be present but could not be identified qualitatively. Variations in current flow were slight and all runs were between 4 and 5 milliamps. All runs except that using stainless steel electrodes indicated other gases which were not identifiable but appeared to be amine types. The lack of any indication of H_2 in the last three runs could be due to a poisoning of the molecular sieve column by one or more of the unidentifiable products. It is also possible that no free hydrogen remained as one of the gases of decomposition since it could have reacted with ammonium ions in the electrolyte.

TABLE I

COMPOSITION OF DECOMPOSITION GASES COLLECTED FOR TWO HOURS AT ROOM TEMPERATURE

Electrode Metal	cc Collected		Identifiable Gases	
	Anode	Cathode	Anode	Cathode
302 S.S.	8	8	N_2	H_2
Copper	14	14	N_2, NH_3	NH_3*
Platinum	12	12	N_2, NH_3	NH_3 *
Silver	15	15	NH_3, N_2	NH_3 *

*Probably H_2 also but could not detect on these runs.

3.0 POLAROGRAM ANALYSIS OF HYDRAZINE AND MONOMETHYLHYDRAZINE

a. Apparatus

Polarographic runs in the 0 to 3 volt range were made using a Heath model EUW-401 polarograph equipped with a Varian millivolt recorder. A platinum and a dropping mercury electrode were used in the electrolytic cell in conjunction with a calomel reference electrode. The polarographs produced in the 4 to 24 volt range were made using the same three electrode system and cell as described in the preceding paragraph. However, input voltage was supplied by 12 volt storage batteries rather than the Heath EUW-401 and current readings were read directly from a milliampmeter incorporated in the circuit.

b. Procedure

Electrolytes for all the polarographs included hydrazine and monomethyl hydrazine with either 0.03% ammonium nitrate or dimethylsulfoxide. Voltage rise rates were varied from 0.05 volts/min to 1.0 volts/min. on the runs in the 0 to 3 volt range, and the rates were automatically regulated through the Heath EUW-401. Polarographs in the 3-24 volt range were controlled manually and voltage was increased in 1 volt/min increments.

c. Discussion

The current-voltage traces for hydrazine and monomethylhydrazine are presented in Figures 2, 3, and 4 on a condensed scale and in step form to emphasize the current plateaus and the critical transition voltages E_{cr}. Figure 2 is a reproduction of an actual polarograph trace. A number of critical transition voltages are observed for both propellants and the current traces of monomethylhydrazine exhibits a 50% decrease as compared with that of hydrazine.

Each critical transition voltage E_{cr} is associated with a particular electrolytic reaction and thus can serve to identify the thermodynamic changes occurring during electrolysis. Ignition criteria, in turn, can be established based on a thermal ignition model where electrolysis data can supply the necessary energy input. Free energy is related to the measured EMF as

$$\Delta F = (0.239)\, n\mathcal{J}E \tag{2}$$

where ΔF = free energy change in calories
n = number of electrons involved in electrolysis
$\mathcal{J}$ = Faraday constant ($\approx$ 96,500 coulamb)
E = measured EMF.

Since the solutions, in general, do not contain ions at unit activity, the free energy is different from the standard free energy and a concentration conversion must be made. The variation of EMF due to the ion concentration is

$$\begin{aligned} E &= E^{\circ} - \frac{RT}{n\mathcal{J}} \log \frac{a+}{a-} \\ &= E^{\circ} - \frac{.059}{n} \log \frac{a+}{a-} \end{aligned} \tag{3}$$

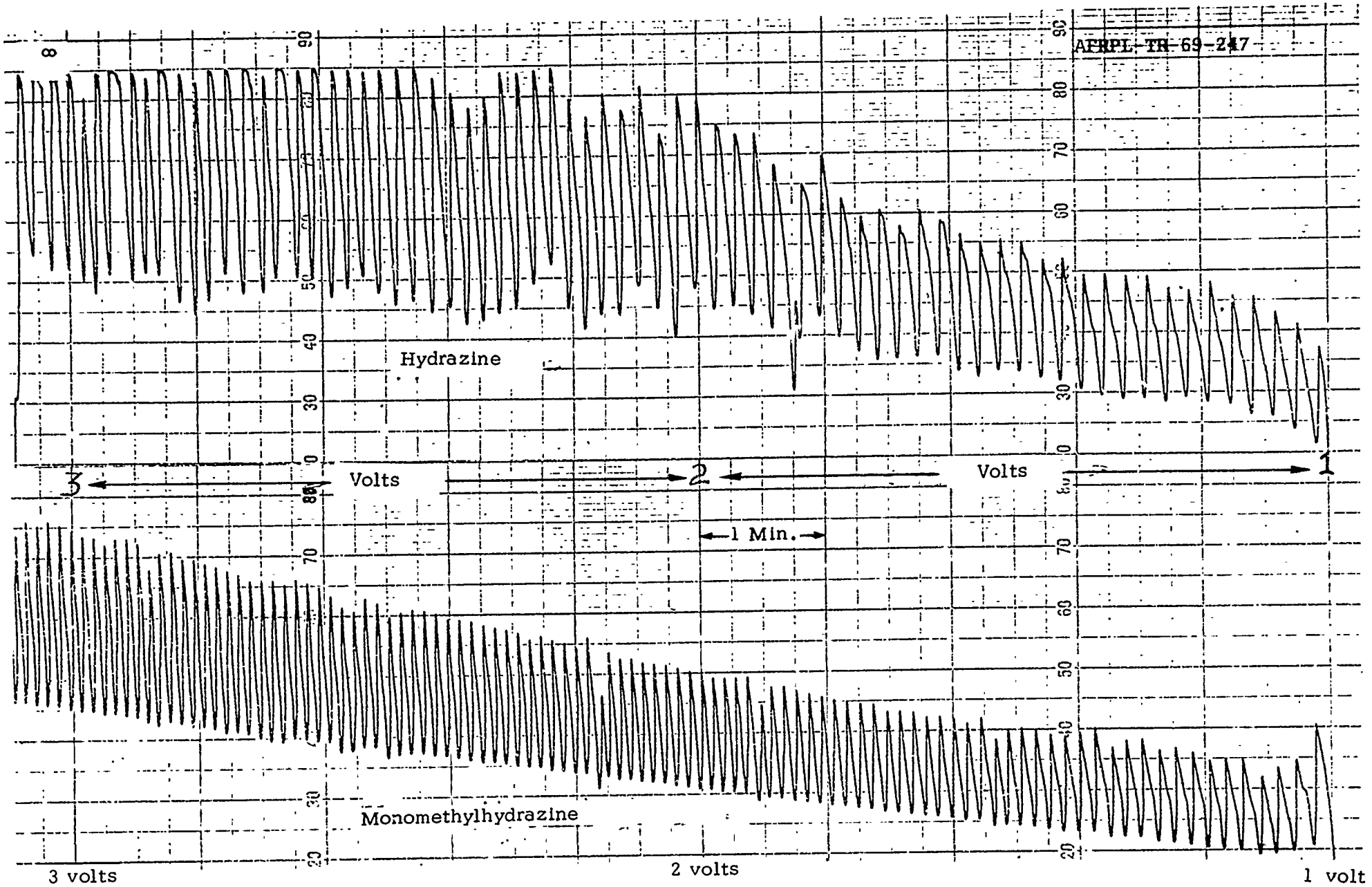

Figure 2. Polarograph Traces of Hydrazine and Monomethylhydrazine
(Initial Potential: 1 volt
Voltage rise rate: 0.2 volts/min)

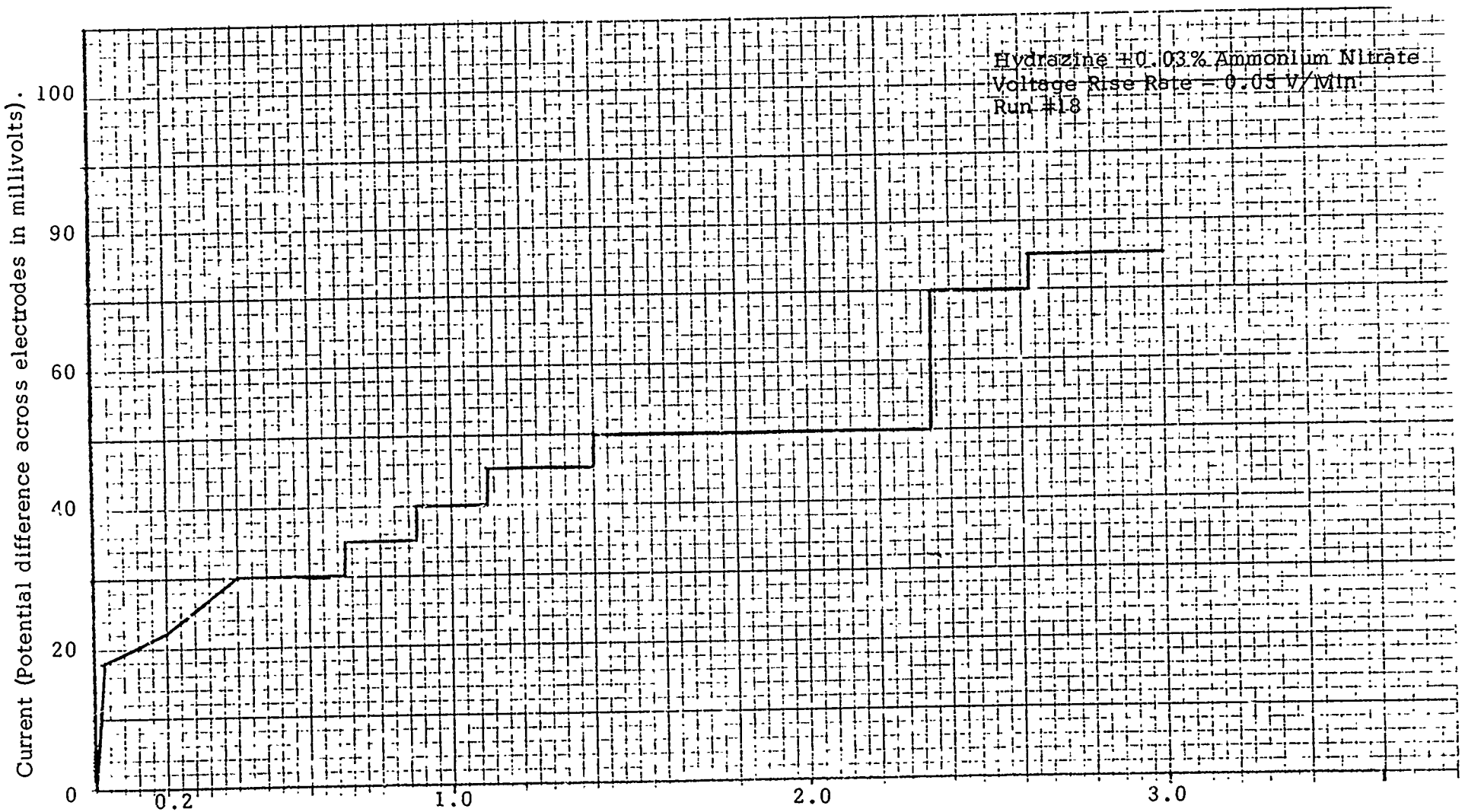

Figure 3. Plot of Voltage/Current trace Volts (Electrolyte-Hydrazine).

MMH +0.03% Ammonium Nitrate
Voltage Rise Rate 0.05 V/Min
Run No. 20

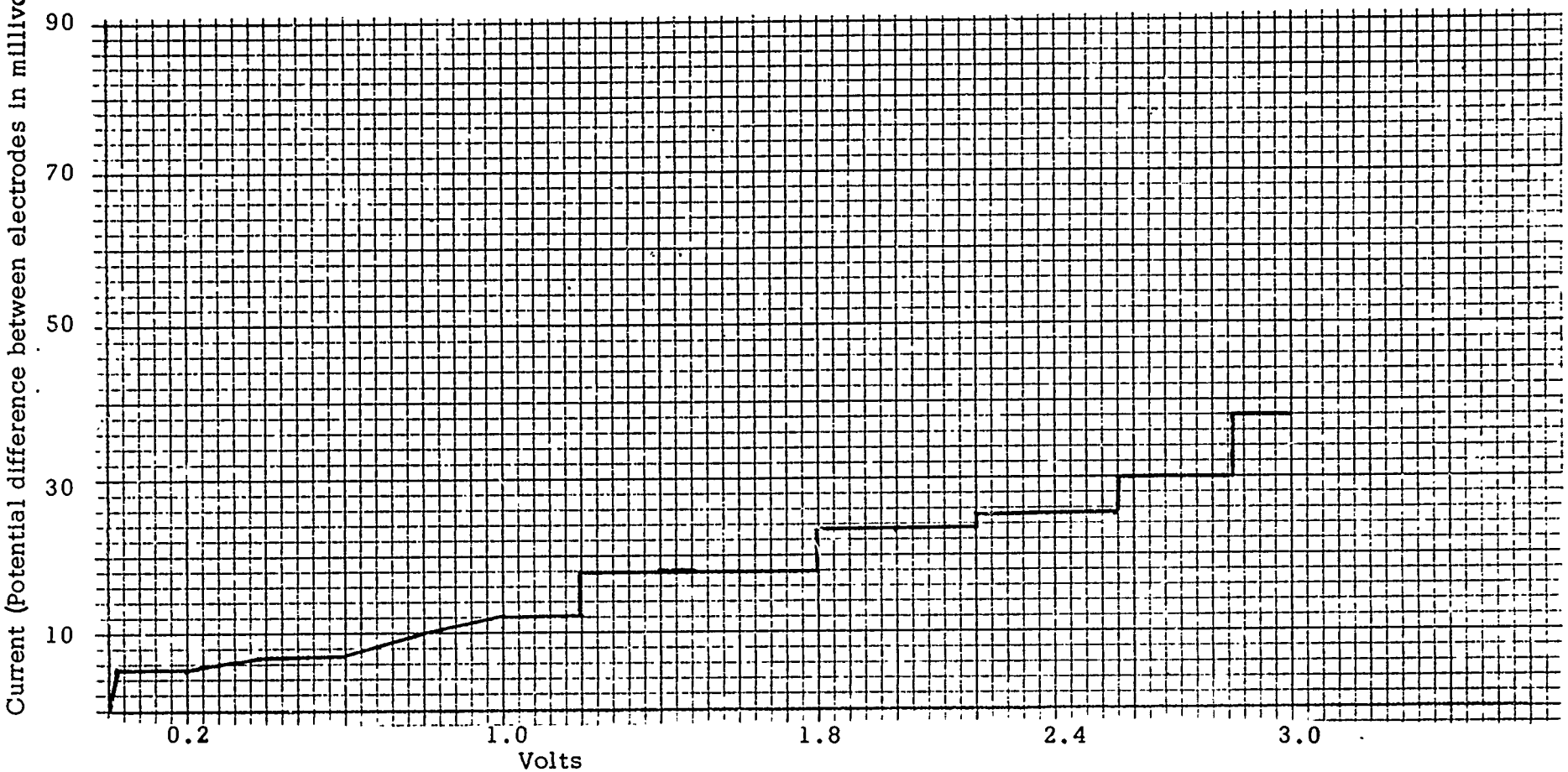

Figure 4. Plot of Voltage/Current Trace (Electrolyte-Monomethyl Hydrazine).

The ion product constant for $2N_2H_4 \rightarrow N_2H_5^+ + N_2H_3^-$ is 10^{-25}. As a first approximation, we will assume that a+ = a- which eliminates the correction term. Even if $C_{a+} = 100\ C_{a-}$, the correction term is only about 0.1 volt which, although not insignificant, can be ignored as a first approximation in the case of hydrazine.

In order to calculate the free energy ΔF, the electron transfer number n has to be defined.

For the reaction: $N_2H_4 \rightarrow 1/2\ N_2 + 1/2\ H_2 + NH_3$, one may take the electron transfer number, n, to be a value of 2. Some comparisons can be made although gross assumptions must be used. In particular, one assumes the electron attachment free energies are the same for all species compared.

The reaction: $NH_2 \rightarrow 1/2\ H_2 + NH$ has a free energy charge of 35 kcal/mole which can be compared with 32.2 in the tabulated data. n=1 is used in this comparison.

The reaction: $1/2\ N_2H_4 \rightarrow NH_2$ has a free energy charge of 24 kcal per mole of NH_2 which can be compared with 25.5 in the tabulated data. n =1 is used in this comparison.

The values of 16.2 and 20.8 in the tabulated data may well compare with reactions involving the parent molecule N_2H_4 but adequate thermodynamic data were not available.

The reaction: $N_2H_2 \rightarrow N_2 + H_2$ has a free energy charge of 58 kcal/mole which may also be compared with 25.5 x 2 = 51 kcal from the table. (n =2 for this reaction).

The electrolytic decomposition of hydrazine could involve reactions of the type

$$\left.\begin{aligned} N_2H_4 &\rightarrow 2NH_2 \\ NH_2 &\rightarrow NH + 1/2\ H_2 \\ 2NH &\rightarrow N_2H_2 \\ N_2H_2 &\rightarrow N_2 + H_2 \\ NH &\rightarrow 1/2\ N_2 + H_2 \end{aligned}\right\} \qquad (4)$$

A path involving $NH_2 + H \rightarrow NH_3$ or stripping of the N_2H_4 molecule could account for ammonia formation.

Based on equation (2), ΔF is calculated for various critical transition voltages and is expressed in Table II.

TABLE II

FREE ENERGY (ΔF) FOR VARIOUS CRITICAL TRANSITION VOLTAGE

Hydrazine		MMH	
E_{cr}	$(\frac{1}{n})$ (ΔF) Kcal	E_{cr}	$(\frac{1}{n})$ (ΔF) Kcal
0.70	16.2	1.20	27.8
0.90	20.8	1.80	41.7
1.10	25.5	2.20	51.0
1.40	32.4	2.56	59.3
2.34	54.2	2.86	66.2
2.62	60.7		

The reference electrode is assumed to be a hydrogen electrode and does not contribute to the EMF except as corrected by the concentration effect which has been neglected.

Polarograph analyses were conducted in the 0 to 3 volt range varying the voltage rise rate. Table III indicates the reproducibility of polarographs within the same voltage rise rate groups. In general, the reproducibility is good. In the case of hydrazine, the first two critical steps appear to be lost at the 0.20 volts/M in rise rate probably due to the loss of resolution in the low voltage range when the voltage is being increased rapidly. A similar explanation may be used to account for additional plateaus at the 0.20 volt/M in rise rate. Plateaus which are very close together may combine at low resolution to produce additional peaks due to overlapping of individual plateaus. The 1.65 peak in several of the runs may be due to an oxygen impurity due to inadequate purging by nitrogen. In any case, from the point of view of a critical condition for electrolysis, the quantitative nature of the plateaus is of less concern than their general location.

TABLE III

E_{cr} VALUES FOR HYDRAZINE AND MMH AT 0 to 3.0 VOLTS

Run No.	Electrolyte*	Voltage Rise Rate Volts/Min	E_{cr}
17	Hydrazine	0.05	0.65, 0.90, 1.15, 1.41, 2.32, 2.60
18	Hydrazine	0.05	0.70, 0.90, 1.10, 1.40, 2.34, 2.62
19	MMH	0.05	1.20, 1.75, 2.25, 2.56, 2.90
20	MMH	0.05	1.20, 1.80, 2.20, 2.56, 2.86
21	Hydrazine	0.20	1.10, 1.42, 1.65, 2.30, 2.58
22	Hydrazine	0.20	1.10, 1.41, 1.60, 2.30, 2.60
23	MMH	0.20	1.30, 1.65, 1.89, 2.0, 2.20, 2.62, 2.80
24	MMH	0.20	1.30, 1.68, 1.90, 2.0, 2.20, 2.60, 2.80

*All electrolytes contain 0.03% ammonium nitrate.

Another series of manual polarographs using a dropping mercury electrode and a platinum electrode were obtained for hydrazine and monomethyl hydrazine in the 4 to 24 volt range using ammonium nitrate and dimethylsulfoxide at .03% as additives. Tables IV and V represent the critical voltage data from these runs.

TABLE IV

CRITICAL HYDRAZINE VOLTAGES AT 4 TO 24 VOLTS

Run No.	Additive	Voltage Range	E_{cr}
1	Ammonium Nitrate	4-12	4.2, 6.0, 8.1, 10.0, 10.6, 12.0
4	Ammonium Nitrate	12-24	16, 18, 24
5	Ammonium Nitrate	4-12	4.2, 6.0, 8.1, 8.5, 10.6, 11.0, 12.0
6	Ammonium Nitrate	12-24	16, 18, 24
13	Dimethylsulfoxide	4-12	5.0, 8.1, 10.0
14	Dimethylsulfoxide	12-24	12.1, 16.0, 19.9
15	Dimethylsulfoxide	4-12	5.5, 8.2, 10.0
16	Dimethylsulfoxide	12-24	12, 15, 20

TABLE V

CRITICAL MONOMETHYL HYDRAZINE VOLTAGES AT 4 TO 24 VOLTS

Run No.	Additive	Voltage Range	E_{cr}
2	Ammonium Nitrate	4-12	4.0, 6.0, 8.0, 12.0
3	Ammonium Nitrate	12-24	14.0, 18.0, 22.0, 24.0
7	Ammonium Nitrate	4-12	4.4, 6.0, 8.0, 12.0
8	Ammonium Nitrate	12-24	14.1, 18.0, 20.0, 22.0, 23.9
9	Dimethylsulfoxide	4-12	4.0, 8.0
10	Dimethylsulfoxide	12-24	18.0, 22.0
11	Dimethylsulfoxide	4-12	4.0, 8.0
12	Dimethylsulfoxide	12-24	18.0, 22.0

Typical hydrazine and monomethylhydrazine current traces are shown in Figure 5, 6, 7, and 8. Again, plots are in step form to emphasize current plateaus and critical voltage transitions. A 100% current increase is observed when ammonium nitrate is added as compared with dimethyl-sulfoxide.

It was the original intention of taking the polarographs to assist in the interpretation of the mechanism of decomposition and, even more important, to establish voltage ranges for efficient operation of the electrolytic ignition cell. After obtaining the polarographs, two facts became apparent. First, the polarograph traces and the detailed decomposition mechanism were too complicated to permit analysis within the scope of the present effort. Efforts to associate voltage plateaus with decomposition energies were not successful. Second, it became evident after obtaining the polarograms, that the decomposition range was well below the voltage needed to provide high currents and rapid electrolysis. It was evident that voltage levels of 24 volts or higher were well above most of the plateaus observed and were certainly adequate to initiate decomposition. In this regard, the polarographs served their most important function - they did show that adequate decomposition could be obtained at voltage levels of practical interest.

An apparent chemical mechanism does seem to fit the observations. The ionization of liquid hydrazine is given by:

$$N_2H_4 \rightarrow N_2H_3^- + H^+$$

$$\underline{H^+ + N_2H_4 \rightarrow N_2H_5^+} \qquad (5)$$

$$2N_2H_4 \rightarrow N_2H_3^- + N_2H_5^+$$

The electrode reactions are:

$$\text{Athode:} \quad N_2H_3^- \rightarrow e^- + 1/2\ N_2 + NH_3 \qquad (6)$$

$$\text{Cathode:} \quad N_2H_5^+ + e^- \rightarrow 1/2\ H_2 + N_2H_4 \qquad (7)$$

The net reaction would correspond to:

$$N_2H_4 \rightarrow 1/2\ N_2 + 1/2\ H_2 + NH_3 \qquad (8)$$

The heat generated by the electrolysis process, as well as the kinetic energy of the ions generates sufficient heat to generate NH_2 radicals which then propagate a thermal reaction.

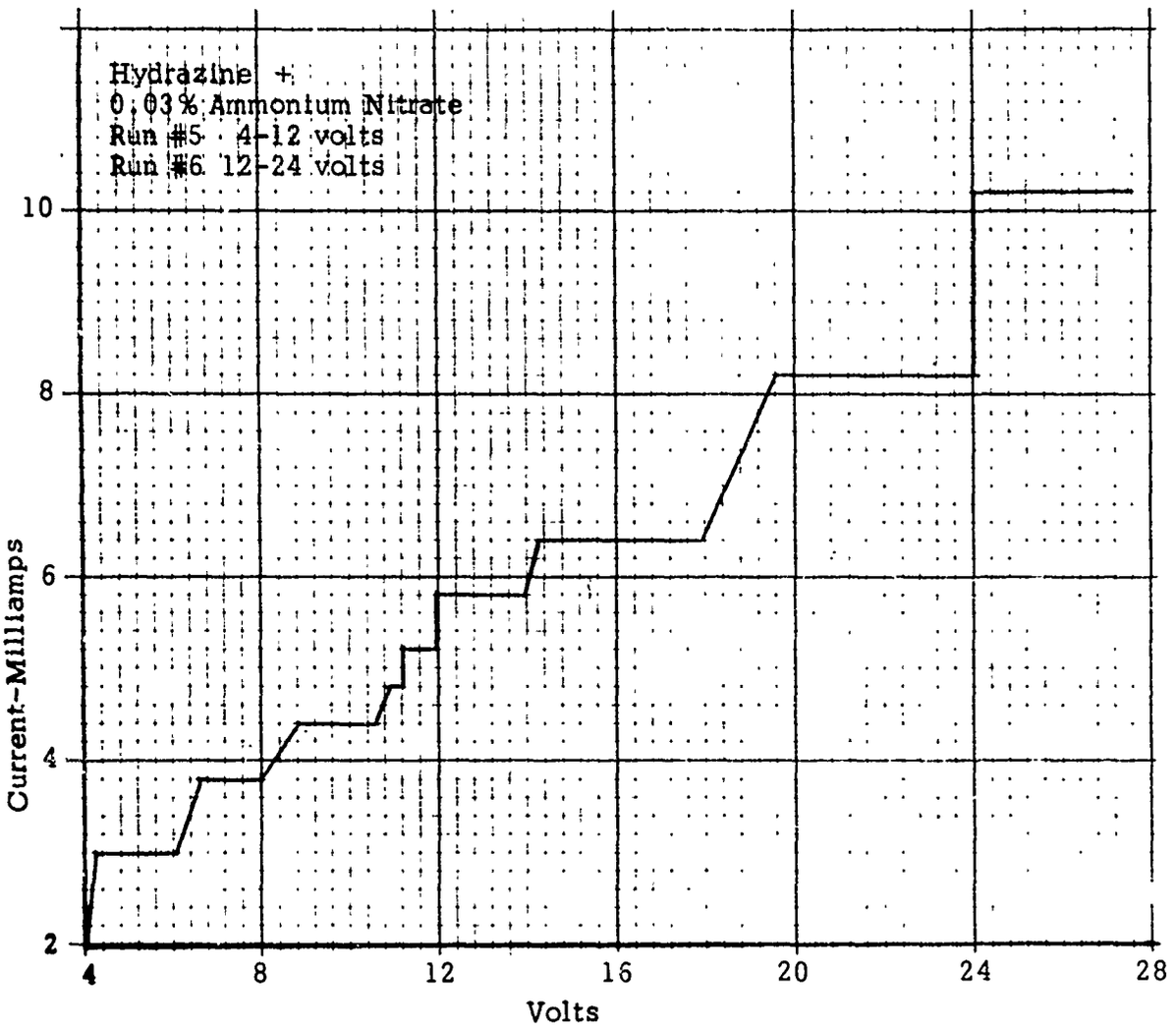

Figure 5. Plot of Voltage/Current Trace (Electrolyte-Hydrazine).

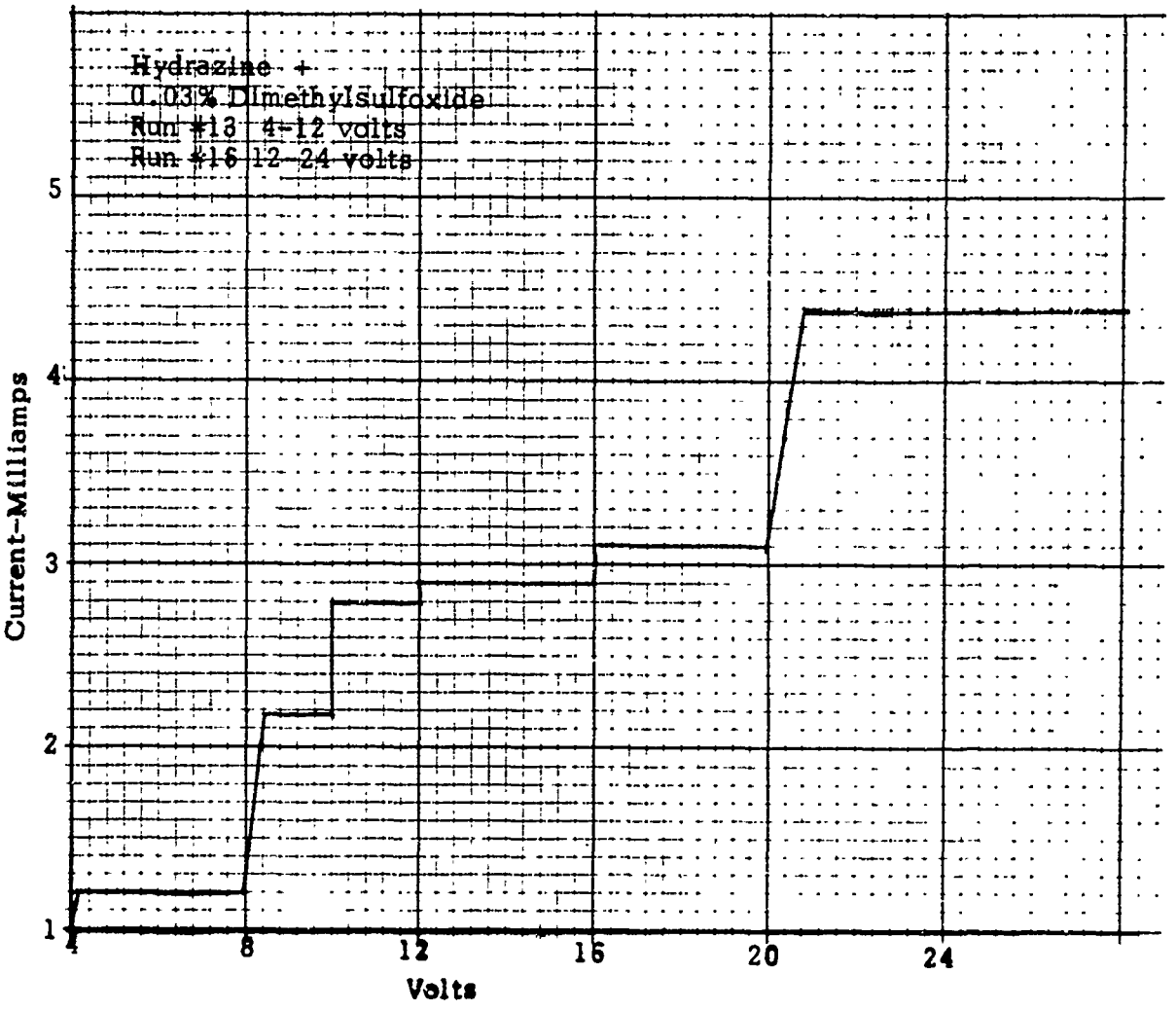

Figure 6. Plot of Voltage/Current Trace (Electrolyte-Hydrazine).

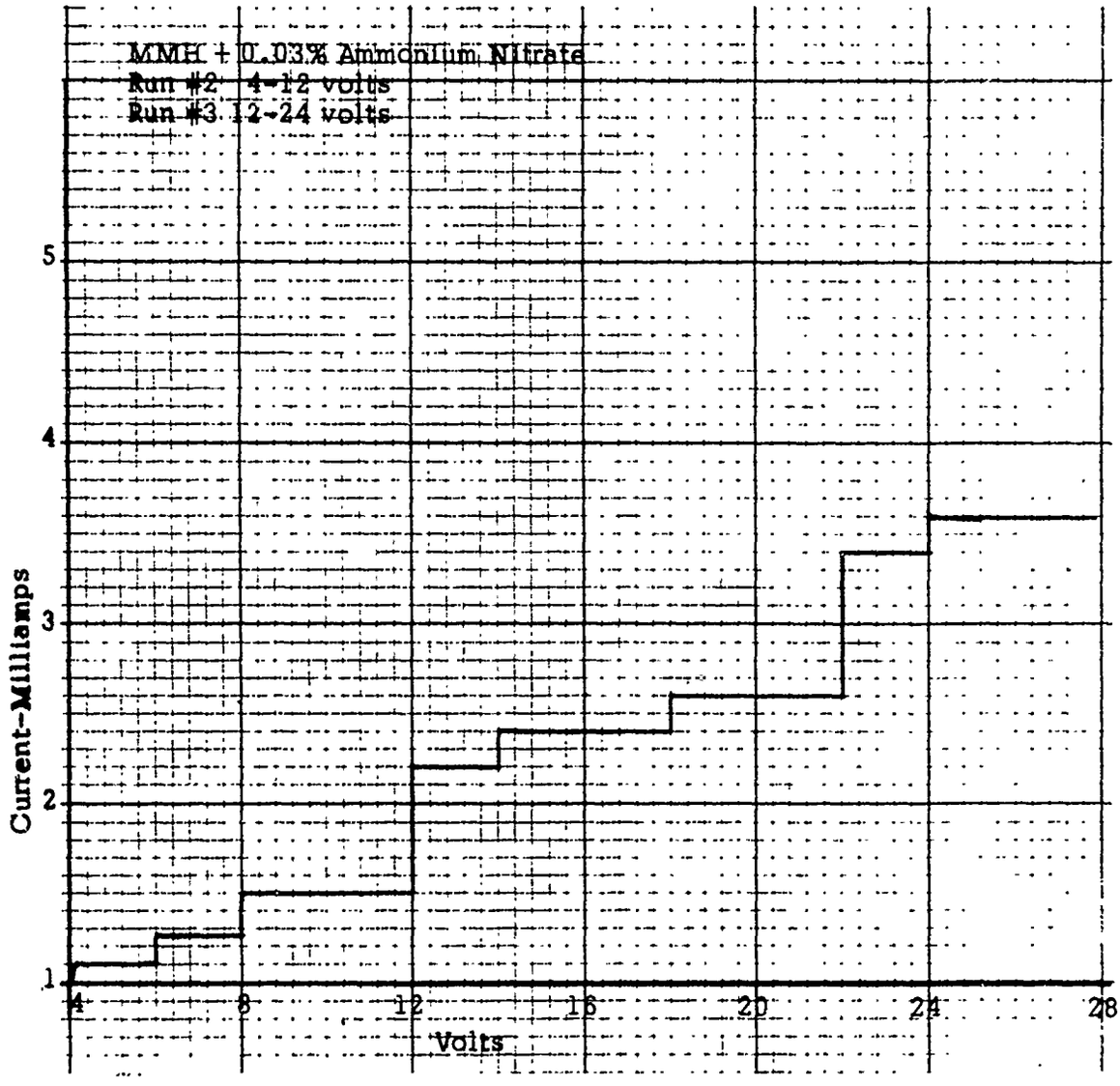

Figure 7. Plot of Voltage/Current Trace (Electrolyte-Monomethylhydrazine.)

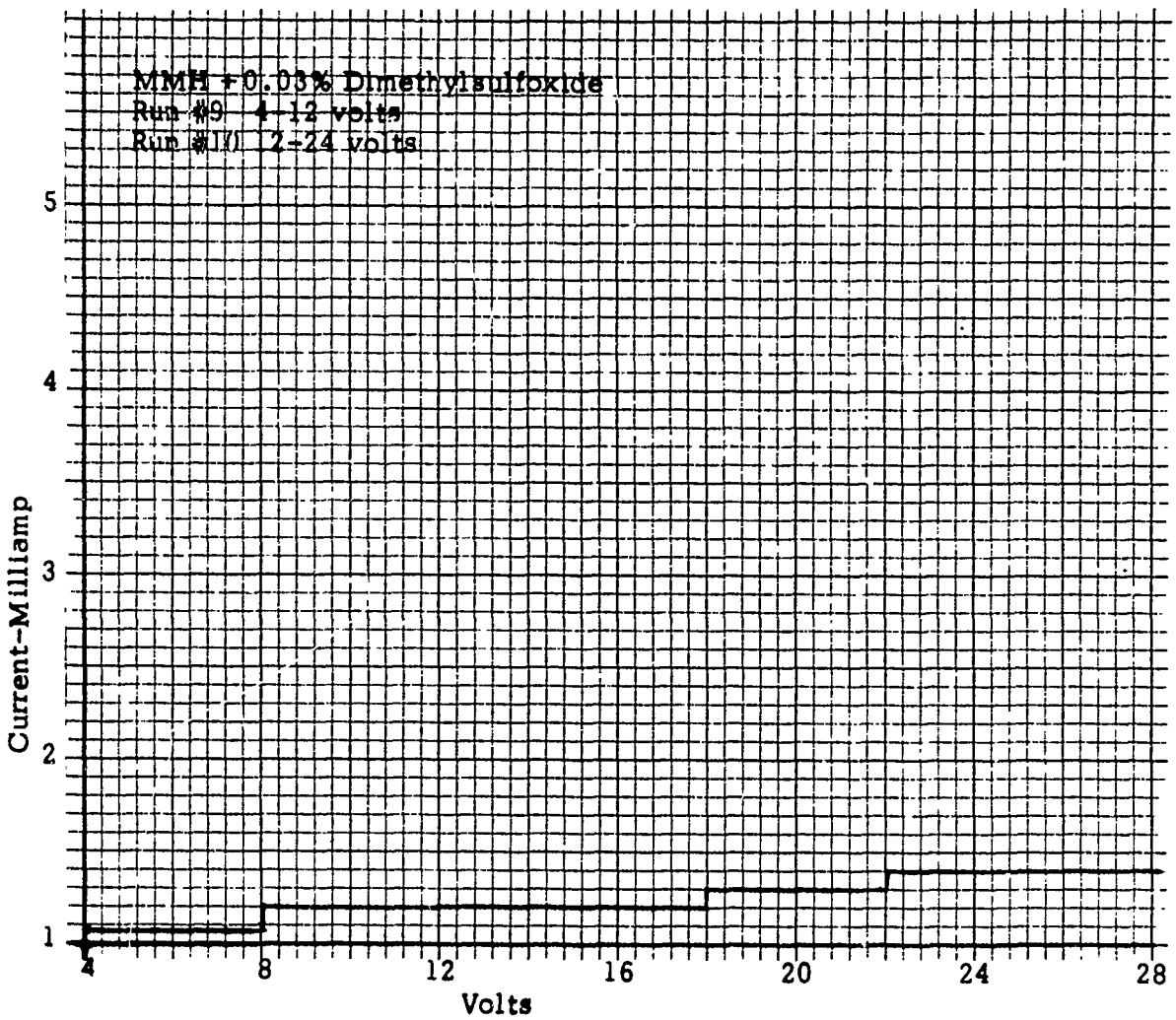

Figure 8. Plot of Voltage/Current Trace (Electrolyte-Monomethylhydrazine).

It is not impossible that the chemical reaction is enhanced by other reactions such as:

$$N_2H_5^+ + e^- \rightarrow NH_2 + NH_3 \qquad (9)$$

Such a reaction would accelerate the monopropellant decomposition by electrolytic free radical generation rather than by heat generation.

The products N_2, H_2 and NH_3 were identified during the electrolysis study but it was not possible to relate the concentrations to specific reactions or combinations of reactions. The polarograph studies suggest that the overall reaction may be quite complex although the initiation reactions associated with the electrode reactions occur in the vicinity of 0.5-2 volts.

4.0 THERMAL IGNITION MODEL WITH ELECTROLYTIC DECOMPOSITION

A simplified concept of thermal ignition of hydrazine induced by electrolysis is being established based on the Semenov theory. The Semenov theory defines ignition in terms of two criteria:

$$\dot{q}_{gain} = \dot{q}_{loss} \tag{10}$$

and

$$\left(\frac{\partial \dot{q}}{\partial T}\right)_{gain} = \left(\frac{\partial \dot{q}}{\partial T}\right)_{loss} \tag{11}$$

The quantity $\dot{q}_{gain}$ is composed of three quantities: ohmic heating $\dot{q}_{ohm}$, heat production due to electrolysis $\dot{q}_{elect}$, and the heat generation due to decomposition of the propellants $\dot{q}_{chem}$. Consider the propellant flows between two parallel electrode plates of equal area A and a gap spacing L. Electrolytic decomposition occurs on the electrode surface raising the electrode surface temperature. Prior to ignition a thermal boundary layer of thickness δ is thus developed within the propellant along the electrode surface. Similarly a thermal boundary layer δ' is developed within the electrode. The boundary layer thickness δ can be expressed as (Ref. 5).

$$\frac{\delta}{\ell} = \frac{4.52}{Pr^{1/3} Re^{1/2}} \tag{12}$$

where $Pr = \frac{\mu c_p}{k}$ and $Re = \frac{U \ell \rho_p}{\mu}$

and

μ = viscosity of liquid propellant

c_p = propellant specific heat

k = thermal conductivity of propellant

U = propellant flow velocity along the electrode

ρ_p = liquid propellant density

The rate of heat production per unit volume due to ohmic heating is $i^2 \rho$ where i is the current density and ρ is the resistivity. For electrode of area A, $i = \frac{I}{A}$ where I is the experimentally measured current. The resistance R is related to ρ by $R = \rho \frac{L}{A}$. Expressed in terms of I and R, $\dot{q}_{ohmic}$ is equal to $I^2 R \frac{1}{AL}$, and the rate of heat production due to ohmic heating within a characteristic volume $A\delta$ is

$$\dot{q}_{ohmic} = I^2 R \frac{\delta}{L} \tag{13a}$$

The rate of mass being liberated due to electrolysis is $\frac{I}{\mathfrak{F} n}$ where $\mathfrak{F}$ is the Faraday constant equal to 96.496 coulombs and n is the number of electron equivalent.

Define ΔH_{chm} as the heat of decomposition per mole, the rate of heat production due to electrolytic decomposition is

$$\dot{q}_{elect} = \frac{I}{\mathfrak{F}n} \Delta H_{chm}. \tag{13b}$$

The rate of heat production due to chemical reactions is

$$\dot{q}_{chm} = c\,\alpha \exp\left(-\frac{E_{act}}{R_g T}\right) \Delta H_{chm}\, A\, \delta.$$

where

c = concentrations of monopropellant in a first order reaction

α = Arrhenius preexponent constant

E_{act} = activation energy

R_g = gas constant

The quantity $\dot{q}_{loss}$ consists of the heat loss to the propellant and the electrode to raise the propellant and electrode temperatures. The heat required to raise the propellant from initial electrode temperature T_o to the temperature T is $\rho_p C_p A\delta \quad (T-T_o)$. For propellant flow velocity U over electrode length ℓ, the rate of heat loss to raise the propellant temperature is $\rho_p C_p A\delta \quad (T-T_o) / \frac{\ell}{U}$. Similarly by defining ρ_e, C_e and δ' as the electrode material density, specific heat and the corresponding thermal boundary layer thickness, the rate of heat loss to raise the electrode temperature is $\rho_e C_e A\delta' (T - T_o) / \frac{\ell}{U}$. The total heat losses are:

$$\dot{q}_{loss} = \left(\frac{\rho_p C_p A\delta}{\ell / U} + \frac{\rho_e C_e \delta' A}{\ell / U}\right)\left(T - T_o\right) \tag{14}$$

Equation (10) can thus be expressed as

$$I^2 R_L \frac{\delta}{} + \frac{I}{\mathfrak{F}n} \Delta H_{chem} + c\,\alpha \exp - \frac{E_{act}}{R_g T} A\delta \Delta H_{chem}$$

$$= \left(\frac{\rho_p C_p A\delta}{\ell / U}\right) + \left(\frac{\rho_e C_e A\delta'}{\ell / U}\right)\left(T - T_o\right) \tag{15}$$

Dividing Equation (15) by δ and defining

$$\dot{q}_1 = \frac{I^2 R}{L} + \frac{1}{\delta}\frac{I}{\mathfrak{F}n} \Delta H_{chm} + c\,\alpha \exp - \frac{E_{act}}{R_g T} A \Delta H_{chm}$$

$$\dot{q}_2 = \left(\frac{\rho_p C_p A}{\ell / U} + \frac{\rho_e C_e A(\delta'/\delta)}{\ell / U}\right)\left(T - T_o\right)$$

variation of $\dot{q}_1$ and $\dot{q}_2$, which are directly proportional to heat gained and heat loss, is shown in the following sketch.

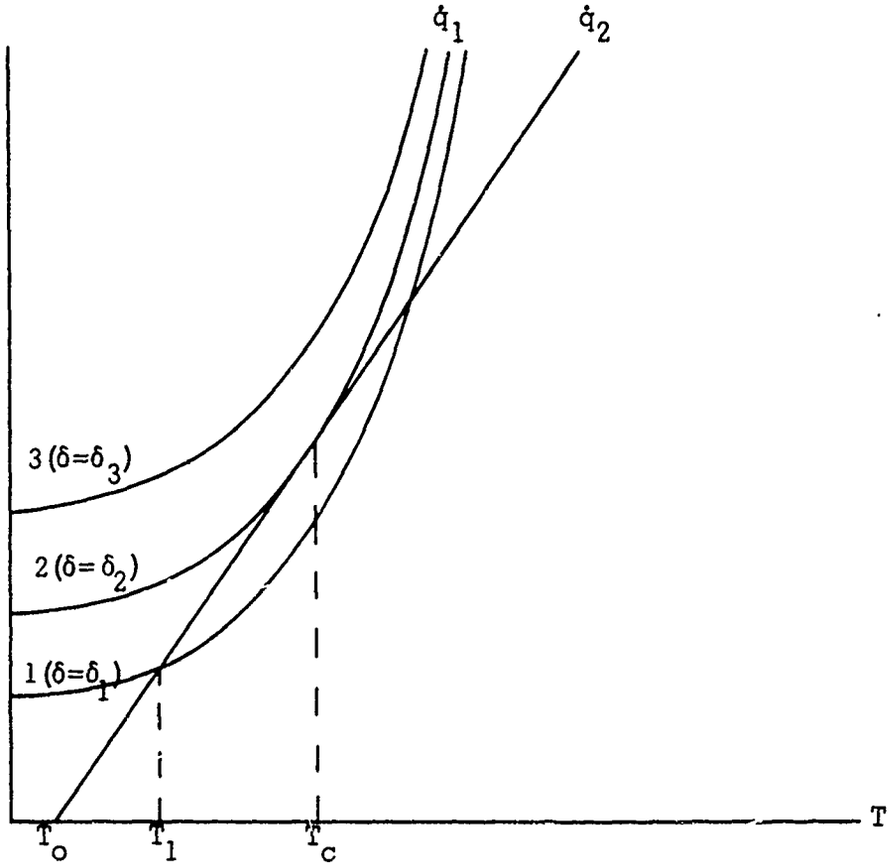

Relation between heat supply $\dot{q}_1$ and the heat loss $\dot{q}_2$ for various thermal boundary layer thickness δ.

For $\delta = \delta_1$, the heat supply $\dot{q}_1$ is at the start larger than the heat removal $\dot{q}_2$. Therefore the electrode surface as well as the propellant within thickness δ_1 become warmer. This continues until the temperature reaches some value T_1 (intersection of $\dot{q}_1$ and $\dot{q}_2$). Then $\dot{q}_1 = \dot{q}_2$. The temperature basically remains constant since for $T > T_1$, the heat removal $\dot{q}_2$ becomes larger than the heat supply $\dot{q}_1$ and if the electrode surface for some reason, would reach a temperature higher than T_1, it would be brought back down to that temperature. Thus for the case $\delta = \delta_1$, ignition does not occur and the propellant and the electrode surface only reaches a temperature T_1, slightly greater than T_o.

For $\delta = \delta_3$, $\dot{q}_1$ does not interact anywhere the straight line $\dot{q}_2$ of heat removal. In this case, the heat supply $\dot{q}_1$ is larger, at all temperatures, than the heat removal $\dot{q}_2$ and thus the electrode surface as well as the propellants within

a thickness δ_3 become continuously warmer, the reaction faster and faster, and ignition takes place.

Curve 2, for $\delta = \delta_2$ is tangent to the line of heat removal at one point T_c and thus define two domains, one where the reaction proceeds in a steady state ($T<T_c$) and the other where ignition takes place ($T > T_c$).

The critical temperature T_c can be obtained based on equations (10) and (11). Based on equation (15), equation (11) assumes the following form:

$$\frac{E_{act}}{R_g T^2}\left[c\alpha \exp - \frac{E_{act}}{R_g T}\right] \Delta H_{chm} = \frac{\rho_p C_p}{\ell / U} + \frac{\rho_e C_e}{\ell / U}\,\frac{\delta'}{\delta} = h \qquad (16)$$

Substituting equation (16) into (15) and define a critical temperature T_c, we obtain

$$\frac{I^2 R}{L} + \frac{I \Delta H_{chm}}{\mathfrak{F} n \delta} + h \frac{R_g T_c^2}{E_{act}} = h (T_c - T_o) \qquad (17)$$

Solving for T_c, one gets

$$T_c = \frac{\frac{E_{act}}{R_g} \pm \sqrt{\frac{E_{act}^2}{R_g^2} - \frac{4 E_{act}}{h R_g}\left(\frac{I^2 R}{L} + \frac{I \Delta_{chm}}{\mathfrak{F} n}\,\frac{1}{\delta} + h T_o\right)}}{2} \qquad (18)$$

When $\frac{4 E_{act}}{R_g h}\left(\frac{I^2 R}{L} + \frac{I \Delta H_{chm}}{\mathfrak{F} n}\,\frac{1}{\delta} + h T_o\right) << 1$ or $m << 1$ the square root $(1-m)^{1/2} \approx 1 - 1/2m$, there results

$$T_c = \frac{1}{h}\left(\frac{I^2 R}{L} + \frac{I \Delta H_{chm}}{\mathfrak{F} n}\,\frac{1}{\delta}\right) + T_o \qquad (19)$$

If the electrical terms are zero, ($I = 0$), then T_o must equal T_c for ignition. As the electrical terms increase, the required value of T_o can decrease since the ohmic and electrolysis heating compensate for the wall losses. In the extreme, the wall temperature could be zero.

The electrical terms are a combination of resistance heating and electrolysis. A high resistance (low salt concentration) increases the effect of ohmic heating relative to electrolysis. A low resistance(high salt concentration)does the opposite. A very high salt concentration, however, might alter the electrode reactions and change ΔH_{chem}.

The model of thermal ignition with electrolytic decomposition is based upon the well-known Semenov (Ref. 6) thermal ignition theory. The principal difference has been the addition of heat generation terms due to electrolysis and electrolytic conduction. The value of T_c, the critical thermal ignition temperature without electrolysis has not been derived. This temperature would have to be obtained from experiment or theoretical calculation of hydrazine monopropellant

thermal decomposition. The model has been used to show how the wall temperature for thermal ignition can be reduced by homogeneous electrolytic heat generation within the liquid. As one might expect, the thermal input from the walls becomes less important as the electrolyses energy input increases. The factors affecting electrolysis rate and therefore electrolysis energy addition are described beginning with paragraph 5.0 of this section.

The analysis can be further extended to define design criteria. For propellant flows between two electrode plates, in addition to the voltage ϵ and the resulting current I, the important parameters are the electrode length ℓ, gap space L, propellant flow velocity U, and electrode materials. To insure fast ignition responses, one criterium is that the liquid propellant temperature should reach T_c within the electrodes. An approximate approach to give an order of magnitude estimate can be carried out based on the thermal boundary layer analysis.

Decomposition first occurs on the electrode surface and the heat liberated raises the temperature of the propellant immediately adjacent to the wall to a temperature T_f which is usually much higher than T_c. The temperature profile across the electrode can be approximated as

$$\frac{T - T_f}{T_o - T_f} = \frac{y}{\delta} \tag{20}$$

T_o being the initial propellant temperature and y is the distance variable perpendicular to the electrode surface. To insure fast ignition transient, the ignition criteria is that $T(y=L/2) = T_c$.

$$\therefore \quad \delta = \frac{T_o - T_f}{T_c - T_f} \frac{L}{2} \tag{21}$$

or

$$\frac{4.52 \quad \ell}{\left(\frac{\mu c_p}{k}\right)^{1/3}\left(\frac{U\ell\rho_p}{\mu}\right)^{1/2}} = \frac{T_o - T_f}{T_c - T_f} \frac{L}{2} \tag{22}$$

Equation (22) gives us the design criteria in terms of electrode length ℓ, gap space L and other characteristic parameters to insure proper electrolytic ignition. T_f can be obtained based on a more detailed analysis or obtained experimentally.

5.0 FACTORS INFLUENCING ELECTROLYTIC IGNITION

a. Current

The principal factor which adds energy to produce ignition is current. One can increase the current by adjusting any or all of the following parameters:

Resistivity (reciprocal of conductivity) - This is a function of the chemistry of the solution and can be changed by adding soluble salts to the solution, independent of whether they participate in electrolysis or not. The lowest resistivity (highest conductivity) is desired compatible with other chemical properties of the solution.

Resistance - The resistance of a given configuration is given by

$$R = \rho \frac{L}{A} \tag{23}$$

where ρ is the resistivity, L is the gap spacing or conductor length and A is the cross-sectional area of the electrodes. Since a minimum resistance is required, it is desirable to have a low value of ρ as indicated above. The geometrical variables L and A can also be adjusted to provide the lowest value of R consistent with other design requirements. It is evident that a large electrode area, A, and small gap I are desirable.

There is probably an optimum value of the ratio L/A. A small value enhances the energy addition but the quenching of reaction - absorption of heat and free radicals - is also favored by a small L/A so that an optimum probably exists.

The last factor available to promote reaction is the voltage. Since the energy is given by $\frac{E^2}{R} t$ (where t = time) it is evident that the highest voltage consistent with other system considerations will favor ignition.

In summary then, the following design guides for electrolytic ignition can be stated:

Voltage	- as high as possible	
Resistivity	- as low as possible	
Gap length	- as short as possible	provided excess quenching
Electrode area	- as large as possible	does not occur.

On the basis of some preliminary experiments, it appears that one joule of energy can cause ignition. A logical system may well be represented by a condenser discharge where the energy is given by $H = 1/2\ CV^2$

where H = energy in joule
C = capacitance in farads
V = voltage in volts

An initial high voltage is available for a high current surge so that the energy is added in short time reducing the heat transfer and other losses and providing the maximum electrolytic effect. The ions produced in the initial surge reduce ρ and promote high currents at the end of the surge when the voltage has decreased.

The electrical energy added is given by

$$\frac{(E + \Delta H_{e\ell})E}{R} t = H_{elect}$$

where $\Delta H_{e\ell}$ is the electrical equivalent in volts of the exothermic heat of decomposition of hydrazine to products.

b. Thermal Factors

Time - Although not a thermal dimension, the heat is generated in the liquid phase. If the electrical energy is added rapidly, less will be lost to the electrodes and other solid surfaces.

Geometry - Low heat capacity of the electrodes and low thermal conductivity is desirable. Shapes of the form:

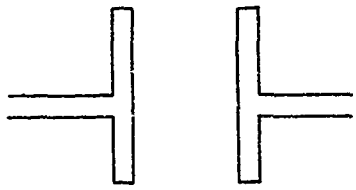

may be desirable if the large flat portions have a very low heat capacity. The large area will promote electrical conductivity through the liquid while the thin leads, adequate for electrical conductivity, will inhibit heat transfer through the electrodes.

c. Fundamentals of Electrolytic Conduction

All of the current passed through an electrolytic cell involves electrolysis. An insignificant exception to this is a small leakage which occurs at voltages below the breakdown potential.

At any potential above the breakdown potential and any over-voltage effects due to polarization, etc., the number of moles of material reacting can be found from:

$$m = \frac{It}{n\mathcal{F}}$$

where

I	=	current
t	=	time
n	=	number of electron equivalents
$\mathfrak{F}$	=	Faraday - 96,500 coulombs

This calculation deals with quantity - nothing here determines the energy balance. A voltage is required to complete the picture.

At some minimum voltage, ideally, electrolysis is initiated and the energy is just adequate to accomplish the necessary chemical changes. The electrical energy added under any conditions is given by EIt

where E = voltage.

If E is in volts, I in amperes and t in seconds, the energy is in joules where

1 joule = 0.239 calories

The chemical reaction, generally but not necessarily, an endothermic reaction absorbs a portion of this energy, a quantity determined on a purely thermodynamic basis. A particular reaction cannot absorb more than the thermodynamic quantity unless some other change occurs, usually a change in temperature.

The chemical energy can be calculated from the heat of reaction where

$$\epsilon_{chem}\, It = \frac{m\Delta H_{chem}}{0.239} \tag{25}$$

The remainder of the energy is used in other ways, principally in heating up the solution. Thus, the energy involved in ohmic heating is given by

$$(E - \epsilon_{chem})\, It = Q_{thermal} \tag{26}$$

Combining eqns. (21) and '22)

$$\epsilon_{chem}(n\ \mathfrak{F}) \times 0.239 = \Delta H_{chem} \tag{27}$$

Note that ϵ_{chem} is not the standard electrode potential except at equilibrium (incipient electrolysis where $\Delta S = 0$) since $n\ \mathfrak{F}\epsilon_{stand} = \Delta F$ and $\Delta F = \Delta E - T\Delta S$.

ϵ_{chem} is little ($T\Delta S$ is relatively small) but not much different from ϵ_{stand}.

d. Endothermic Reaction

In the case of an endothermic reaction, the quantity $n\ \mathfrak{F}\epsilon_{chem}$ joules are used for the chemical process. The quantity given by equation

or by

$$EIt - \epsilon_{chem}\, It = Q_{thermal} \tag{28}$$

or

$$EIt - \frac{m\Delta H_{chem}}{0.239} = Q_{thermal} \tag{29}$$

is used for heating.

e. Exothermic Reaction

In the case of an exothermic reaction, the quantity $n\,\mathfrak{F}\,\epsilon_{chem}$ is actually given off so that

$$EIt + \frac{m\Delta H_{chem}}{.239} = Q_{thermal} \tag{30}$$

or

$$EIt + \epsilon_{chem}\, It = Q_{thermal} \tag{31}$$

also

$$\left(E + \frac{\Delta H_{chem}}{n_e \mathfrak{F} 0.239}\right) It = Q_{thermal} \tag{32}$$

The energy absorbed in initiating the exothermic chemical reaction is like an activation energy and is returned to the system as heat at the end of the reaction.

$\dot{Q}_{thermal}$, or the rate of heat addition is given by $I(E + \epsilon_{chem}) = \dot{Q}_{thermal}$

$\dot{Q}_{chemical}$, or the rate of chemical reaction independent of electrolysis is given by

$$\rho V \Delta H_{chem} f(c) e^{-E/RT} = \dot{Q}_{chem} \tag{33}$$

A heat balance would then look like

$$I\,(E + \epsilon_{chem} + \rho V \Delta H_{chem} f(c) e^{-E/RT} + c_p \frac{dT}{dt} = \lambda \frac{dT}{dx} \tag{34}$$

The resistance of the solution determines the relationship between E and I, since E = IR even for electrolytic processes.

$$\dot{Q}_{thermal} = \left(E + \frac{\Delta H_{chem}}{0.239\ n_e \mathfrak{F}}\right) \frac{E}{R} \tag{35}$$

In conclusion, the following effects of design and operating variables have been established from the analytical study:

(a) Ignition occurs more readily and with shorter delay as the electrode voltage is increased. It is desirable, therefore, to operate at the highest voltage possible within restrictions imposed by the system.

(b) The highest levels of conduction, low resistance, also favor ease of ignition. High conduction can be achieved by the addition of salts or by geometric changes such as increasing electrode area and/or decreasing gap spacing.

(c) High current levels also favor ignition. This effect can be considered as a combination of conclusions (a) and (b) since the current is increased by having high values of voltage and high conductivity.

Although quantitative calculations cannot be made without additional data, it is evident that the heat generation varies as the voltage squared and inversely as the first power of the resistance.

All of the current is carried by electrolysis. The ratio of electrochemical heat release to ohmic heat release is given essentially by the ratio: $\epsilon/(E + \epsilon)$. One can maximize the proportion of heat release due solely to electrochemical processes by decreasing E provided E remains greater than ϵ. This can be done but the rate of electrolysis and hence $\dot{Q}$, the rate of heat addition, will also decrease unless the conductivity of the solution is increased in proportion to the square of the decrease in E.

This analysis has provided the necessary guide lines for the design and testing of typical cells. Additional calculations would have been of limited accuracy and would have been beyond the scope of the present effort.

An important distinction should be made as a part of these conclusions. All of the current, including ohmic heating, is the result of electrolysis. This differs from previous systems like the resistojet where current is used to heat a metallic conductor which then provides a purely thermal source and no electrolysis. In the thermal model, the resistojet concept would be described by the situation where $T_w = T_c$ since no electrolysis occurs. In the electrolytic ignition cell, the heating due to resistance in the lead wires and circuits is negligible and does not contribute to heating or ignition. The only reason for separating the electrochemical process and the ohmic heating process in the electrolysis ignition discussion was to provide an understanding of the mechanism. It is not really possible to separate the energy used to generate an ion from the kinetic energy of that ion when formed. In the electrolytic ignition cell this kinetic energy is not wasted since it is converted into heat.

SECTION III

FEASIBILITY STUDIES OF HYDRAZINE MONOPROPELLANT ENGINE

1.0 ELECTROLYTIC IGNITION OF HYDRAZINE (Cup Tests)

a. Test Procedures

Electrolytic ignition was accomplished in air and under nitrogen cover in a stagnation system consisting of a 1.5 cc capacity plexiglass cell equipped with two flat surfaced stainless steel electrodes 1/4 inch in diameter and placed 1/16 inch apart (Figure 9a). The cell was affixed in a metal enclosure equipped with a nitrogen purge system and a safety glass view window (Figure 9b). Voltage was supplied through a simple circuit using storage batteries. Initial experiments using this equipment were made in order to ascertain apparatus reliability and electrolytic ignition of hydrazine did occur. However, reproducibility was not adequate with 1/16 in electrode gap. Testing was monitored using a scope ammeter and voltmeter (Figure 10). A photocell circuit was added to the system in order to record time and scope of ignition as well as amperage during the test runs. Photographs were taken of the oscilloscope traces and the reduced data from these photos are tabulated in Table VI.

(1) Electrode Rods: The electrodes for runs 1 through 27 were stainless steel rods 0.1040 inches in diameter and 0.25 inches long. The electrolyte for all runs was 1.5 cc of hydrazine/20.0% ammonium nitrate. The electrode gap was approximately 0.0008 inches. The small gap spacing, 0.0008 inch was difficult to control. Variations in this value probably account for some of the data scatter. A micrometer attachment was added to provide more precise gap control. Good reproducibility of ignitions was obtained at an input voltage of 48 volts. However, runs No. 20, 22, and 25 show the feasibility of ignitions at inputs of 36 and 24 volts. Figures 11, 12, and 13 are actual oscilloscope traces of representative runs at various voltages.

(2) Concentric Electrodes: Ignition experiments were made using the electrode configuration as shown in Figure 14a. Successful ignitions were obtained using the concentric electrode-configuration; however, shorting was pronounced between the outer screen and inner core. No instrumentation tests were made during these runs.

(3) Flat Screen Electrodes: Two types of flat screen electrodes were used similar to those depicted in Figure 14b. The first trials were made with single screens 1-1/2 inch long and 1/4 inch wide. Again, ignitions were successful using 48 and 36 volt inputs but the screens frequently buckled and shorted against one another. Double screens 1-1/2 inches long and 1/4 inch wide were prepared in an attempt to increase the rigidity of the electrodes under voltage loads as well as increase the electrode area. Instrumented test runs were made at input voltage of 48, 36, 24, and 12 volts respectively. The screens were separated by a mica strip to prevent either shorting of or arcing between electrodes and the electrode gap for all runs was 0.035". Repeated successful ignitions were obtained at all input voltages but those at 12 volts were not dependable. Reduced data from the oscilloscope traces are tabulated in Table VII.

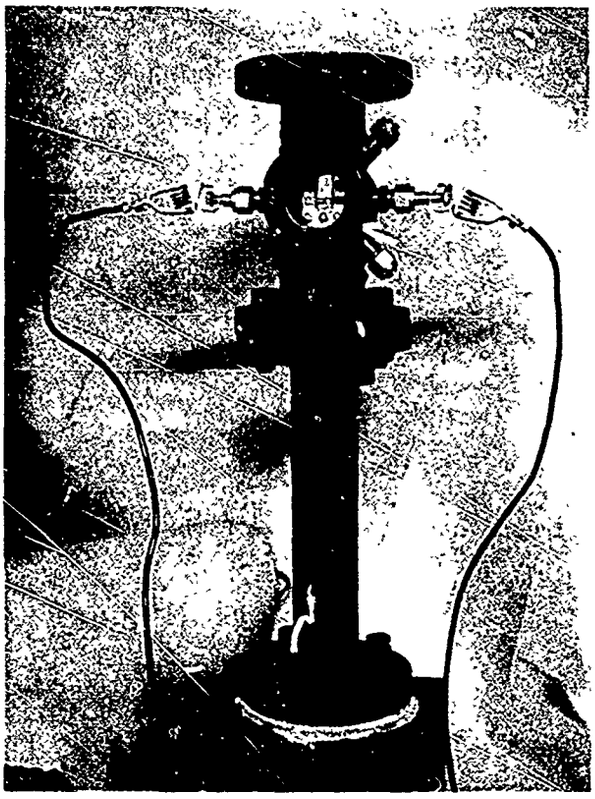

COMPLETE ASSEMBLY

PLEXIGLASS CELL

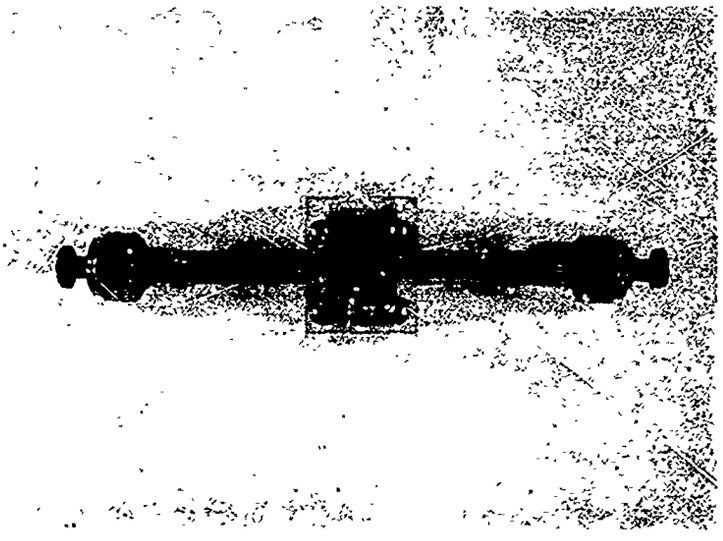

Figure 9. Hydrazine Electrolytic Ignition System

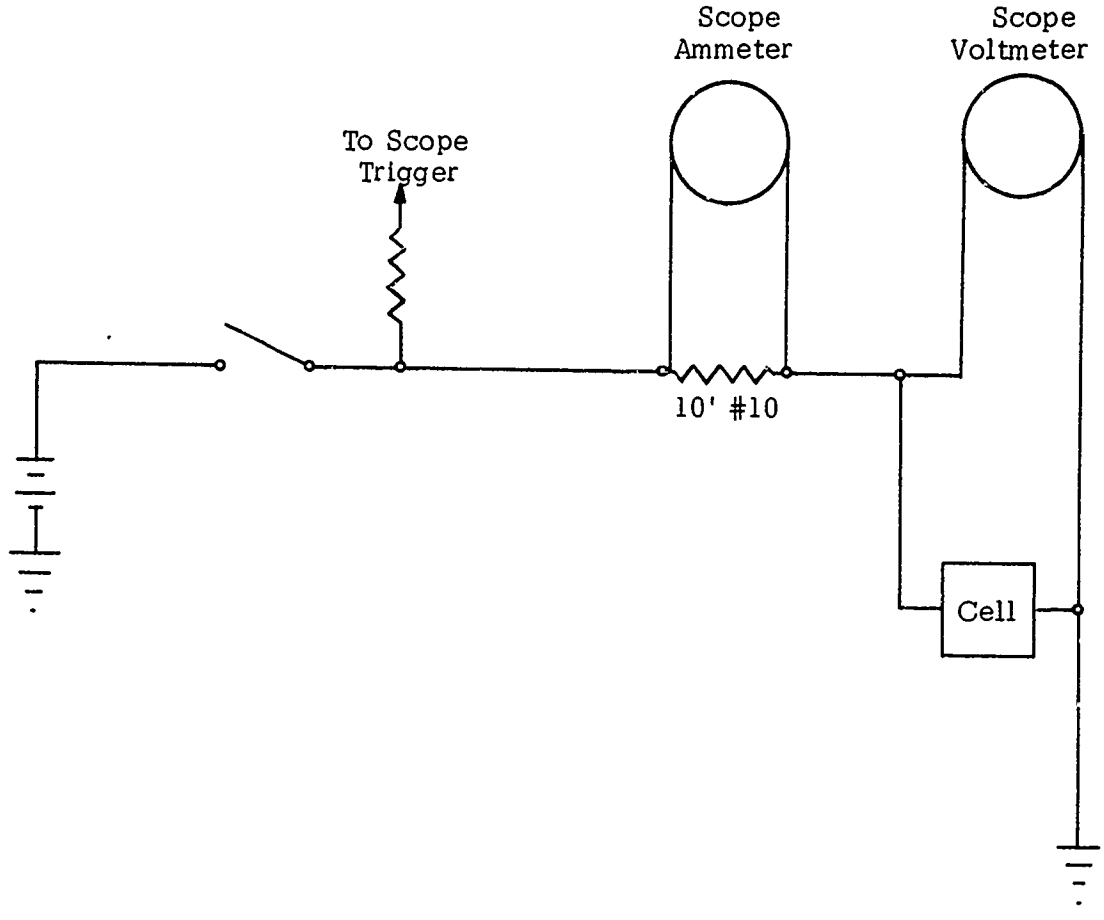

Figure 10. Schematic of Electrolytic Ignition Circuit with Monitoring Instrumentation.

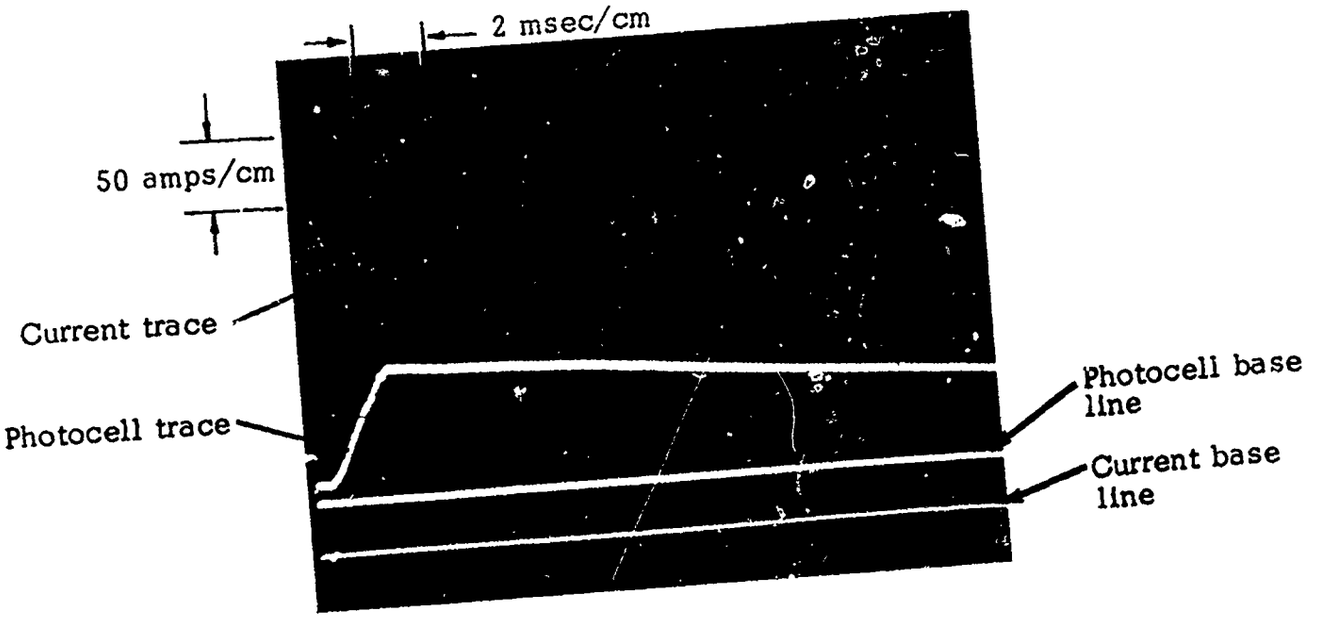

Run #1, 76 volt input

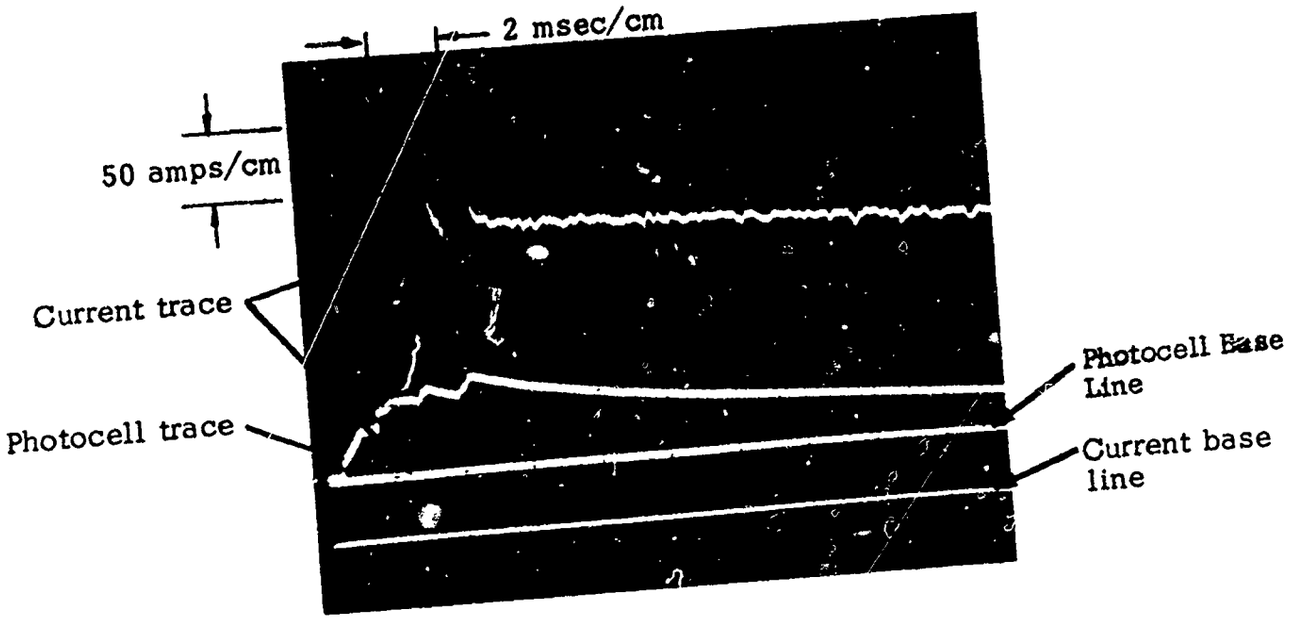

Run #25, 24 volt input

Figure 11. Oscilloscope Traces of Electrolytic Ignition of Hydrazine

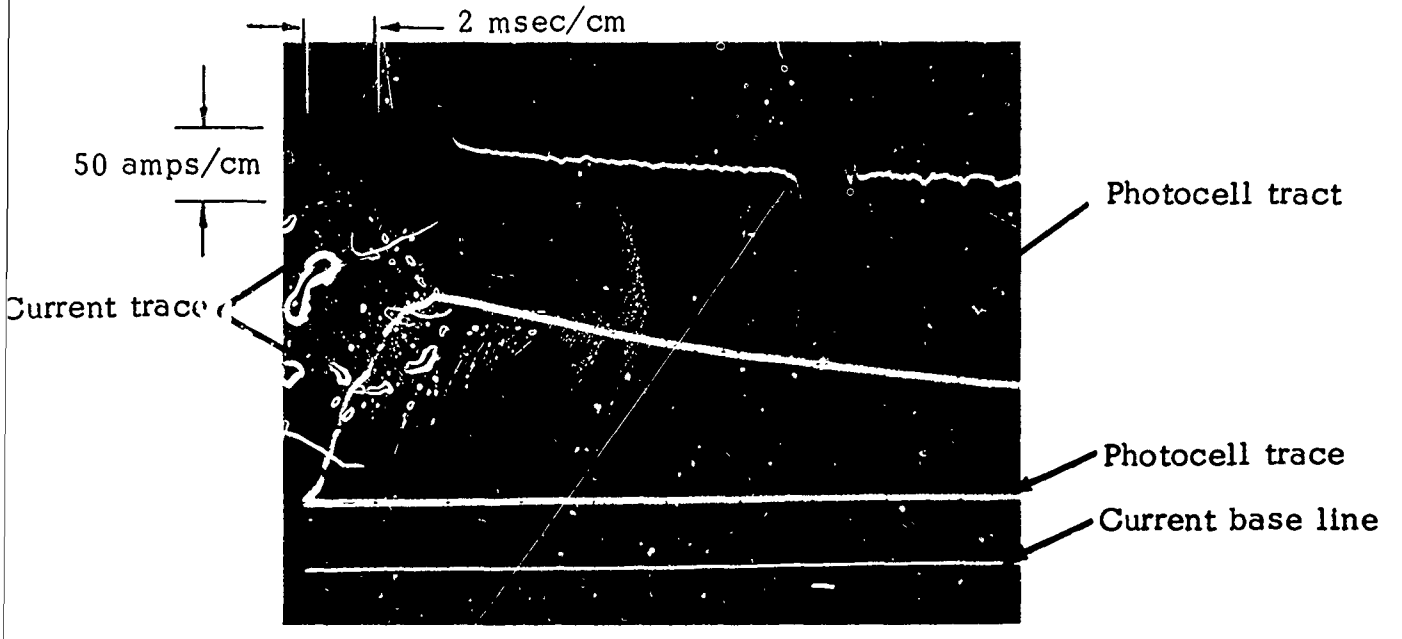

Run #20, 36 volt input

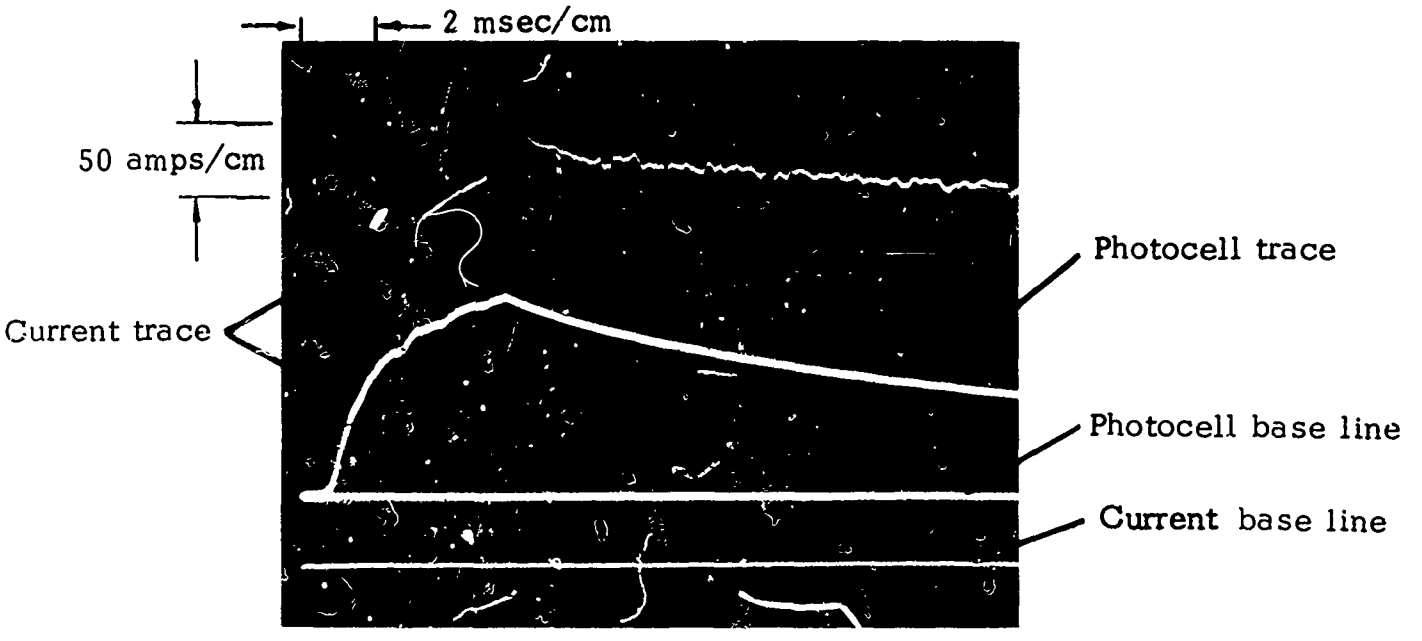

Run #22, 36 volt input

Figure 12. Oscilloscope Traces of Electrolytic Ignition of Hydrazine

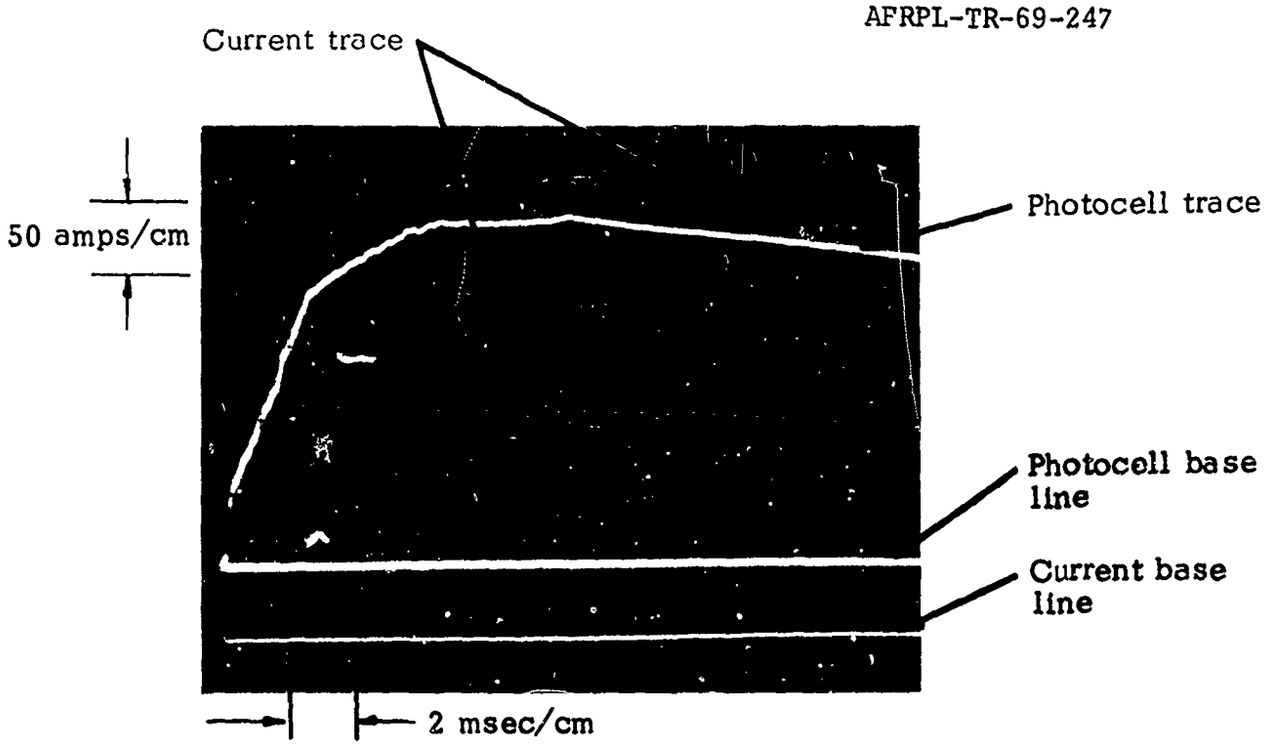

Run #9, 48 volt input

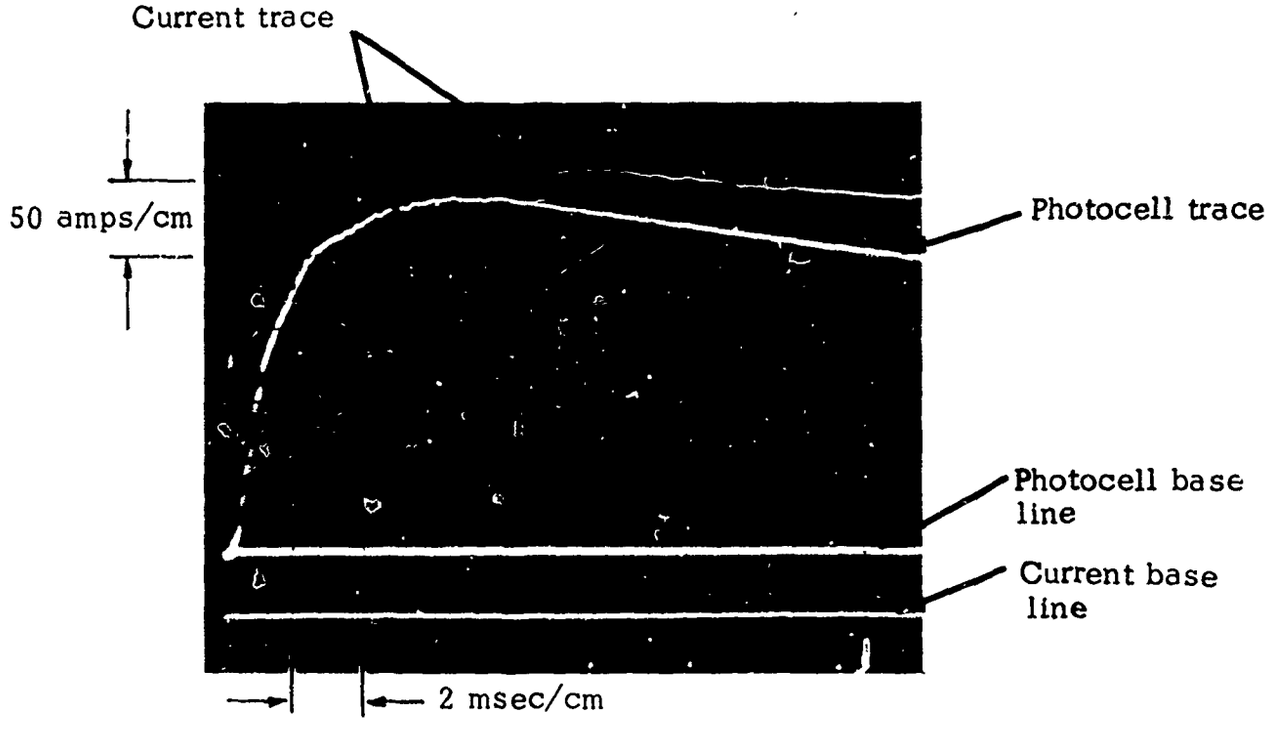

Run #10, 48 volt input

Figure 13. Oscilloscope Traces of Electrolytic Ignition of Hydrazine

TABLE VI

IGNITION DATA FROM STAINLESS STEEL ELECTRODE RODS IN STATIC SYSTEM

Run No.	Input Voltage	Time to Appearance of Light (msec)	Current at Ignition (amps)	Peak Current (amps)	Photocell Peak Reading (volts)
1	76	1.50	270	270	10.8
2	76	No ignition	Electrode short		
3	48	No ignition		310	1
4	48	No ignition	Electrode short		
5	48	No ignition	Electrode short		
6	48	No ignition	Electrode short		
7	48	No ignition	Breaker blew	225	
8	48	0.10	100	200	22
9	48	0.05	100	175	24
10	48	0.20	150	300	24
11	48	0.20	150	310	24
12	48	No ignition	Breaker blew	225	
13	48	1.90	150	310	24
14	48	0.40	175	310	20
15	48	13.8	310	310	25
16	Bad photo - could not reduce data				
17	48	0.20	225	225	11
18	36	No ignition	Electrode short		
19	36	No ignition		50	
20	36	0.20	100	275	14
21	36	No ignition	Flash only	50	
22	36	1.00	113	275	14
23	24	No ignition	Electrode short		
24	24	No ignition	Electrode short		
25	24	0.60	125	215	7
26	24	No ignition		215	
27	24	No ignition		215	

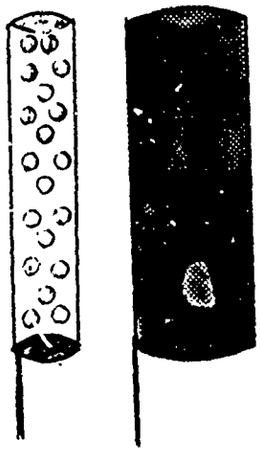

Cylindrical screen outer electrode
Semi-solid core electrode

A

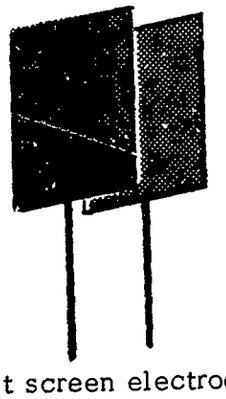

Flat screen electrodes

B

Figure 14. Electrode Configurations.

b. Discussion

One can analyze the ignition data on the basis of:

$$Q_{elect} = \left(\frac{E^2}{\rho}\right)\left(\frac{A}{L}\right)t \qquad (36)$$

If a critical (assumed constant) value of Q_{elect} is required for ignition, then for a given electrode geometry (A/L constant) and a given electrolyte (ρ constant) one can write

$$t = kE^{-2}$$

where

$$k = (Q_{elect})\left(\frac{\rho L}{A}\right)$$

or

$$\ell nt = -2\,\ell nE + \ell nk$$

A plot of log t vs log E is illustrated in Figure 15 where a line of slope-2 has been drawn through the data. A reasonable correlation results. The data used were:

Voltage	Average time, msec
76	0.6
48	1.66
36	2.1
25	4

The data presented show that hydrazine ignition by electrolysis can be obtained repeatedly. At higher voltages, between 36 and 72 volts, the gap spacing is less critical and ignition is obtained quite reproducibly. At lower voltages, 24 and 36 volts ignition can be obtained provided the electrode geometry is carefully controlled. As shown in the discussion of electrolysis fundamentals, the gap geometry represented by (A/L) electrode area divided by gap spacing can be used to vary ignition characteristics and to bring the voltage down to 28 volts for short ignition times.

The data in Tables VI & VII may be used to establish correlations. On the basis of the equations

$$R = \frac{E}{I} \quad \text{and} \quad \rho = R\,\frac{A}{L} \qquad (37)$$

a value of $\rho = 4.355$ ohm-inches is calculated for the specific resistivity. In a somewhat more conventional manner, the specific conductivity corresponds to 0.23 mho/in or 0.09 mho/cm. Salt solutions in water have specific conductivities of the order of 0.2 mho/cm for similar salt concentrations. Since water is a better conductor and a better ionizing solvent than hydrazine, the value of 0.09 for hydrazine solutions seems quite reasonable.

TABLE VII

IGNITION DATA FROM TESTS USING DOUBLE SCREEN ELECTRODES*

Run No.	At Ignition: Time (MS/cm)	At Ignition: Current (V/cm)*	At Ignition: Current (amps)	Photo Cell Intensity (V/cm)	Input Voltage (Volts)	Ignition Time (Millisec)
1	0.1	1	200	.5	48	0.12
2	0.1	5	500	.2	"	0.42
3	0.1	5	500	.2	"	0.30
4	0.1	5		.05	"	Missed Ignition
5	0.1	2	100	.05	"	0.1
6	0.1	2	200	5	"	Missed Ignition
7	0.1	2	500	5	"	0.18
8	0.1	2		10	"	Double Ignition (Missed 1st) 2nd at 0.65
9	0.1	2	400	20	"	0.25
10	0.1	2	420	20	"	0.125
11	0.1	2	420	5	"	0.125
12	0.1	2	410	2	"	Double Ignition (Missed 1st) 2nd at 0.25
13	0.1	2	600	2	"	0.4
14	0.1	2		1	"	Missed Ignition
15	0.1	2		1	"	Missed Ignition
16	50 μa	2	500	1	"	70 μa (microsec)
17	0.1	2		.5	"	Missed Ignition
18	0.2	2	600	.5	"	0.45
19	0.2	2	600	.5	"	0.075
20	0.1	2	600	.5	"	.15
21	0.1	2	400 & 400	0.5	36	Two Ignitions 0.25 and 0.5
22	0.1	2	400	0.5	"	0.025
23	-	-	-	-	-	Intensity too great
24	0.1	0.5	off scale (over 300 Amp)	1	"	0.125
25	0.1	0.5	"	1	"	Missed Ignition
26	0.1	0.2	"	0.1	"	Ignition Bad
27	0.1	0.2	"	0.1	"	0.075
28	0.1	0.1	"	0.1	"	0.025
29	0.1	0.05	"	0.05	"	0.075
30	0.1	0.05	"	0.05	"	0.025
31	0.1	0.05	"	0.05	"	0.2
32	0.1	0.05	"	5	"	0.225
33	0.1	0.05	"	.5	"	Missed Ignition
34	50 μa	0.05	"	.5	"	25 μa (microsec)

*Surface area of each electrode equals 1.5 sq. in.

* Oscilloscope reading proportional to current.

TABLE VII (Continued)

Run No.	Time (MS/cm)	At Ignition Current (V/cm)*	At Ignition Current (amps)	Photo Cell Intensity (V/cm)	Input Voltage (Volts)	Ignition Time (Millisec)
35	20 μa	0.05	off scale (over 300 Amp)	.5	36	84 μa (microsec)
36	0.1	0.05	"	.5	"	0.025
37	0.1	0.05	"	.5	"	0.2
38		Missed Ignition Got Flame				
38A	0.1	0.05	off scale	.5	"	0.17
39	0.1	1.0	550	.5	"	0.09
40	0.1	1.0	600	.5	"	0.09
40A	0.1	1.0	550	.5	"	0.32
41	0.1	1.0	600	0.1	24	0.15
42	0.1	1.0	600	0.1	odd shot	Can't read
43	0.1	1.0	500	.05	24	0.125
43A	0.1	0.5	off scale	0.5	24	0.05
44		Ignition but scope intensity too great				
44A	0.1	0.5	?	.05	24	0.15
45	0.1	0.05	25	.5	24	0.075
46	0.1	0.05	off scale	0.5	24	0.075
47	0.1	0.05	off scale	0.5	24	0.15
48	0.1	0.5	65	0.5	24	0.05
49	0.1	.5	75	0.5	12	0.05
50			Too intense		12	
51	0.1	0.5	50	0.5	12	0.02

*Oscilloscope reading proportional to current.

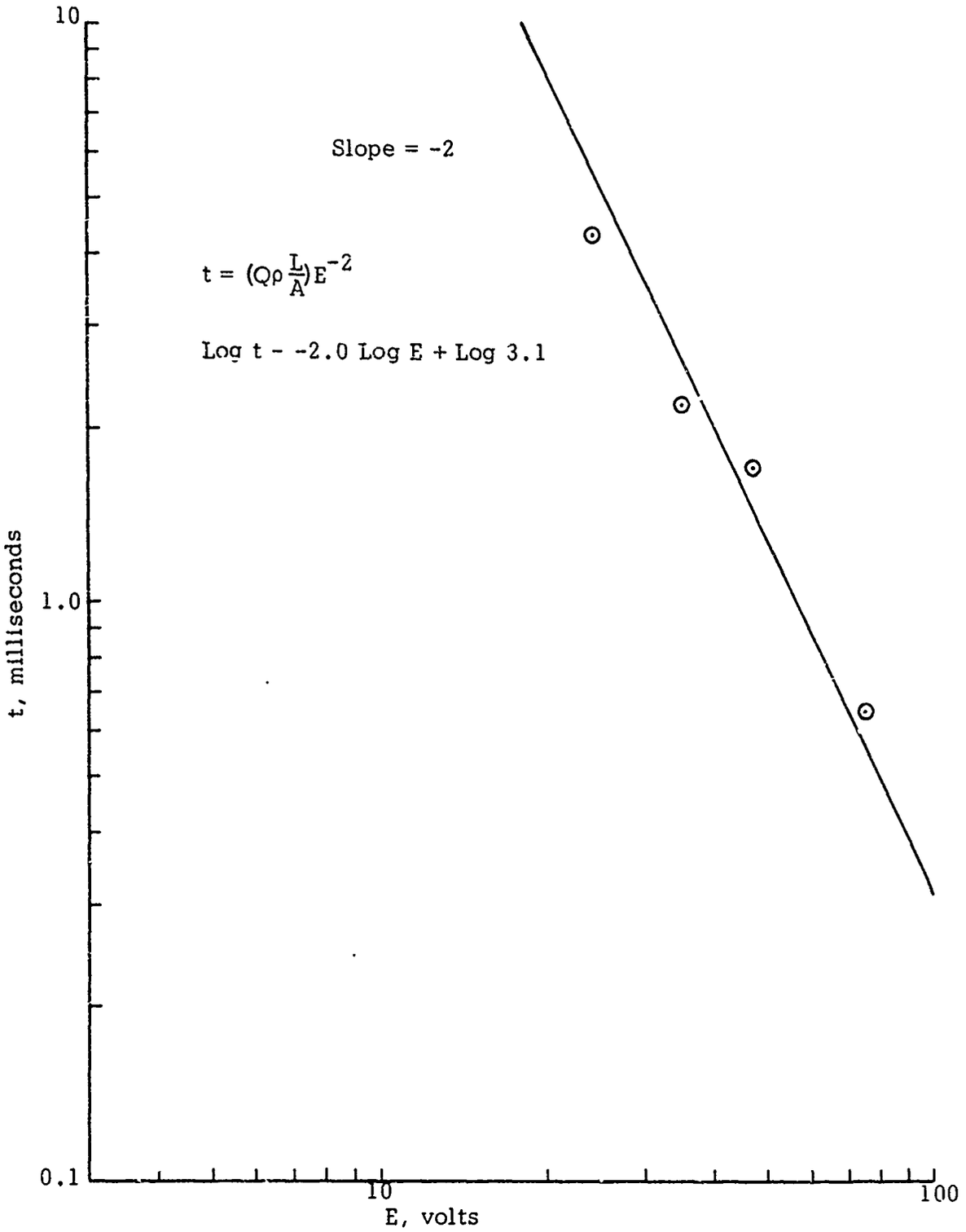

Figure 15. Log t versus Log E.

One may now calculate $(E+\Delta H_{e\ell})E/R$ which corresponds to $\dot{Q}_{thermal}$, the thermal equivalent of the energy added by electrolysis. This has been done for the data of Tables VI and VII.

The results of $\dot{Q}$ vs E are shown in Figure 16. A line of slope 2 based on $\dot{Q} \approx E^2$ has been drawn through the data. The difference in the two sets of data is due to the difference in R between the two configurations. Figure 17 shows the variation of $\dot{Q}$ with E for the average of the experimental data. The graph in Figure 18 shows the effect of variation in $\Delta H_{e\ell}$ on the slope and location of the line. A value of $\Delta H_{e\ell} = 1.0$ corresponds to 23,000 calories/mole. It is evident that $\Delta H_{e\ell}$ has very little effect on the general trends within reasonable values of heats of decomposition.

The variation of $\dot{Q}$ with wattage (EI) is shown in Figure 19. Although the power level is high, the time is short so that the total energy in watt-seconds is still small. For millisecond ignition delays, the energy level corresponds to 1 to 100 joules. Ignition energies of the order of 10 joules and above are presently used in jet aircraft.

The effect of wall temperature on ignition can be deduced from the relationship between T_w and T_c. An equation of the form:

$$T_w = T_c - a\tau \tag{38}$$

may be used to describe the data. Experimental results from a prior study are shown in Figure 20. An equation of the form:

$$T_w = 428 - 28\tau \tag{39}$$

relates wall temperature to ignition delay.

The ratio of intrinsic to ohmic heating is given by $\Delta H_{e\ell}/E$. Both are due to electrolysis. The heating associated with $\Delta H_{e\ell}$ represents the minimum and is, unfortunately, associated with low current and therefore very low reaction rates. This ratio can be maximized by operating at levels of E near to but larger than $\Delta H_{e\ell}$. This does not maximize heating, however, as illustrated in Figure 20. $\dot{Q}$ decreases with increasing $\Delta H_{e\ell}/E + \Delta H_{e\ell}$ or with $\Delta H_{e\ell}/E$.

From the equation

$$\dot{Q} = \frac{(E+\Delta H_{e\ell})\, EA}{\rho L} \tag{40}$$

it can be seen that $\dot{Q}$ or the heat generation varies directly with A or with the ratio A/L. This result can be useful in scaling engines.

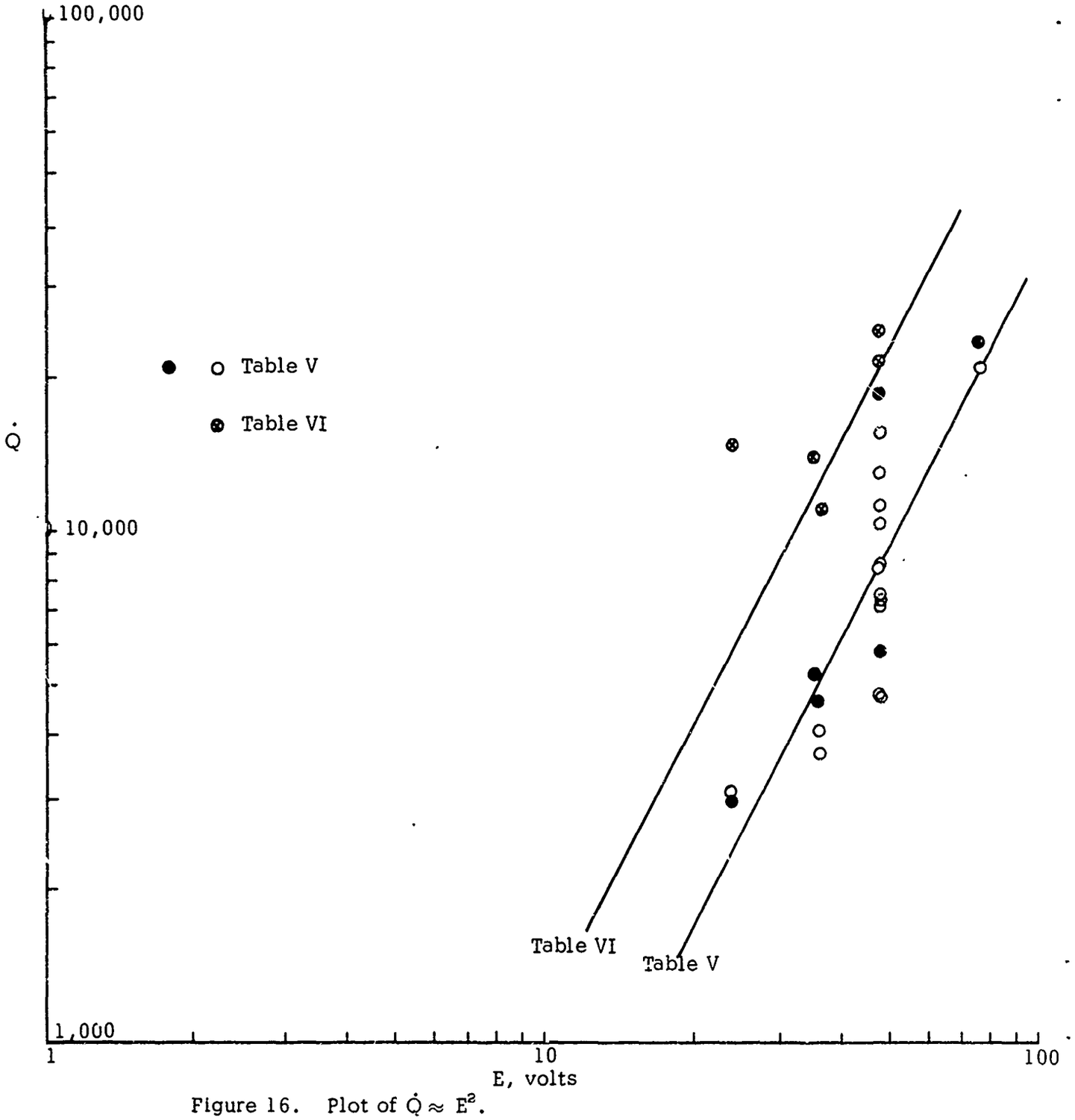

Figure 16. Plot of $\dot{Q} \approx E^2$.

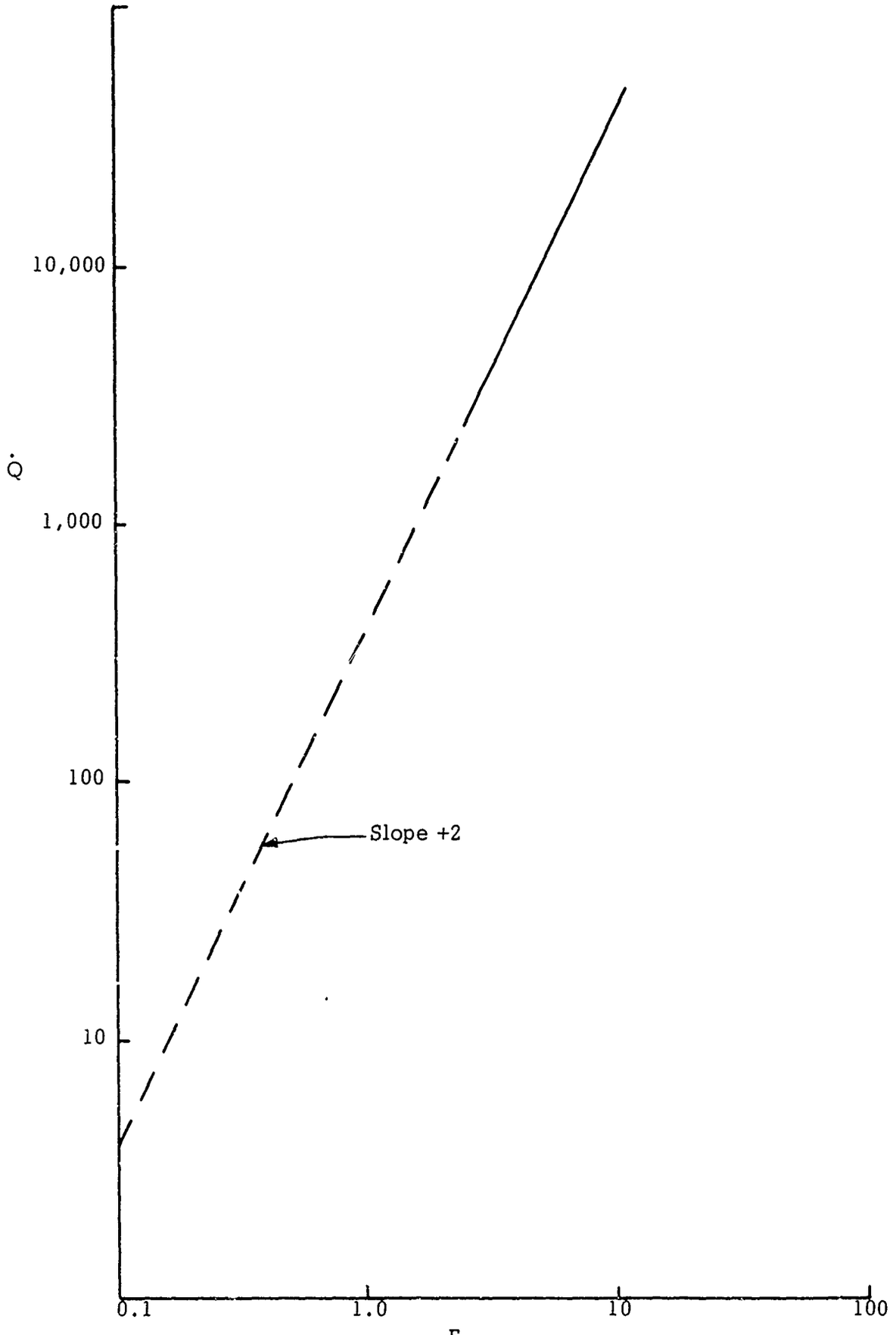

Figure 17. Variation of $\dot{Q}$ with E for the Average of Experimental Data.

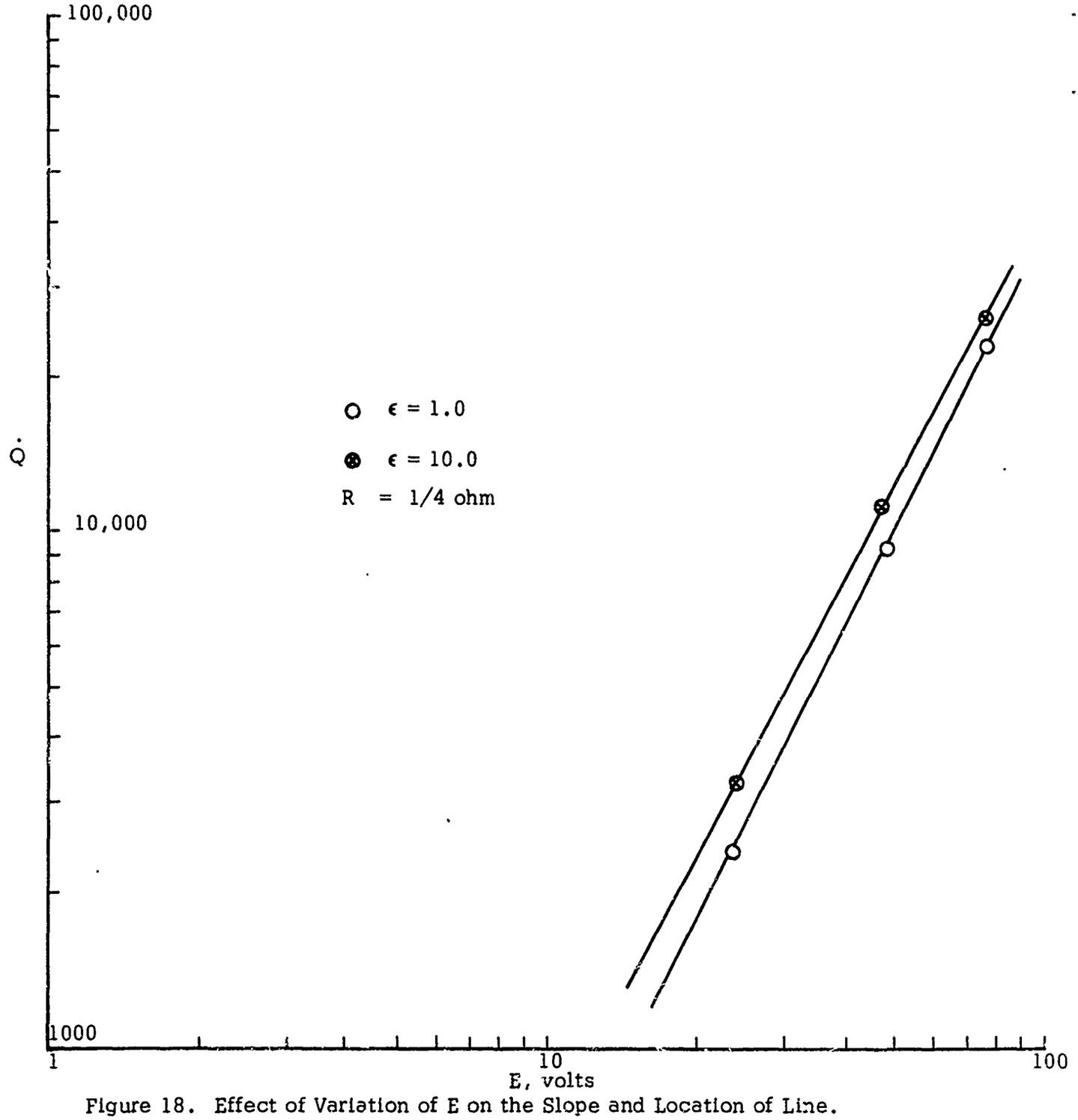

Figure 18. Effect of Variation of E on the Slope and Location of Line.

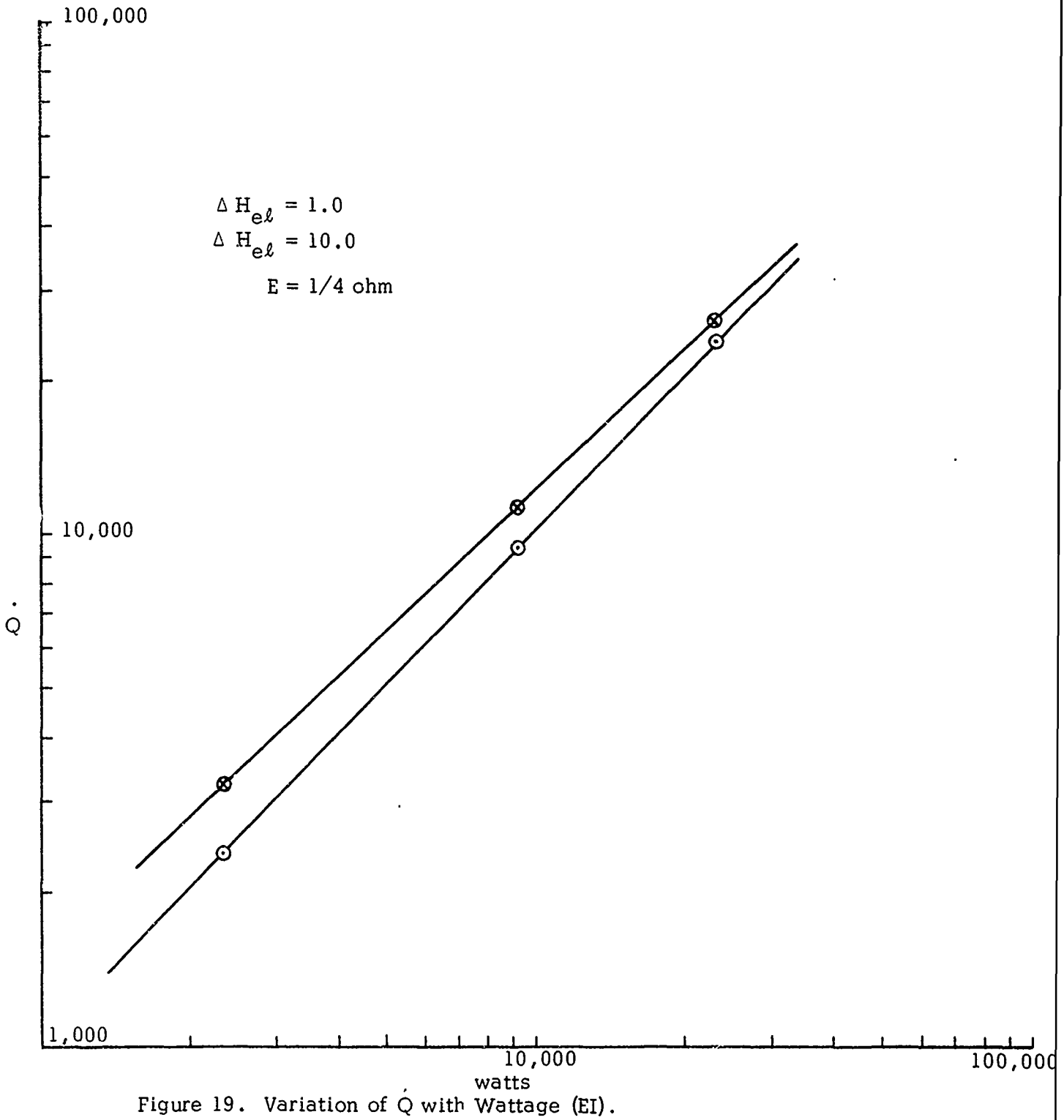

Figure 19. Variation of Q with Wattage (EI).

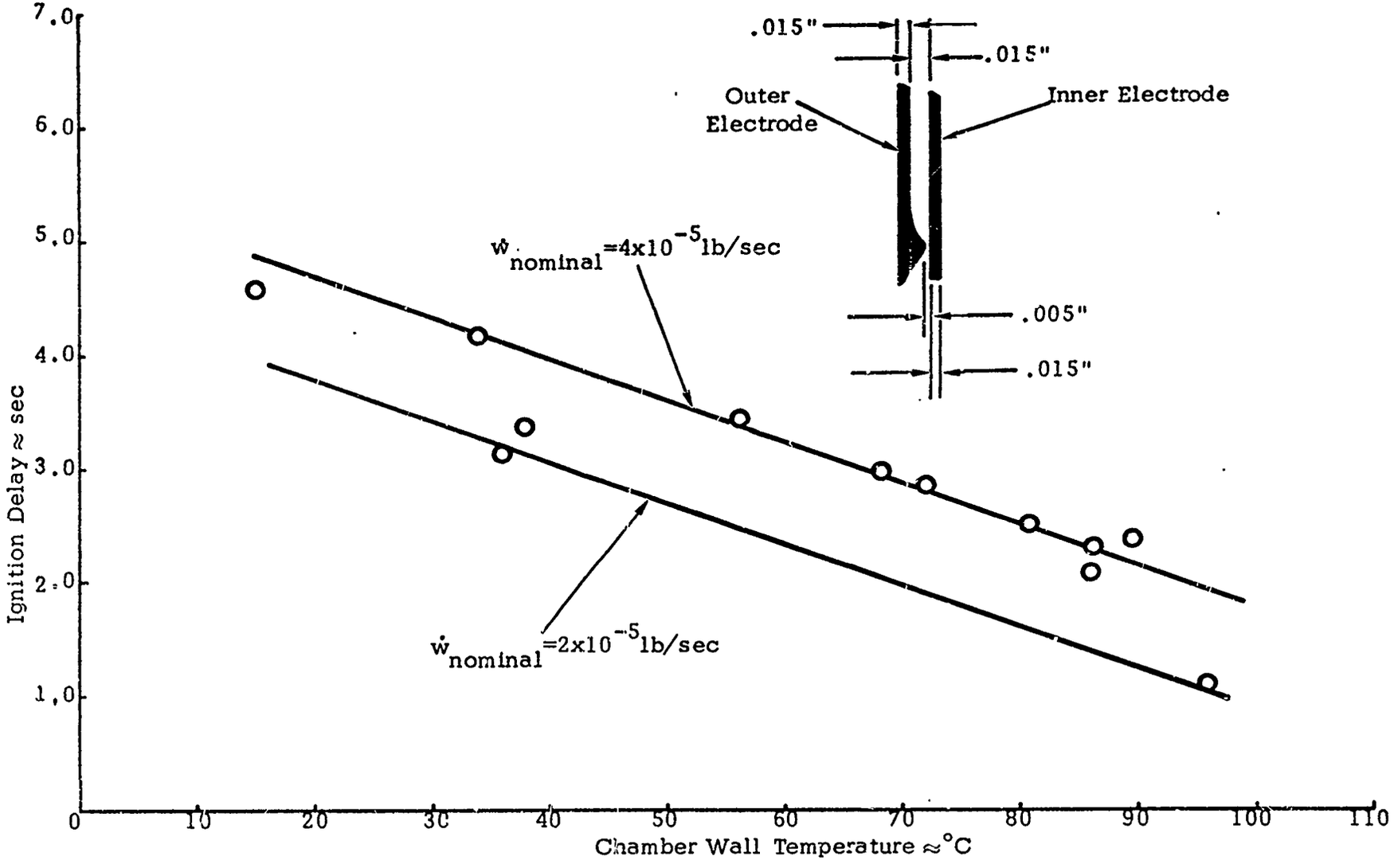

Figure 20. Effect of Temperature on Ignition Delay

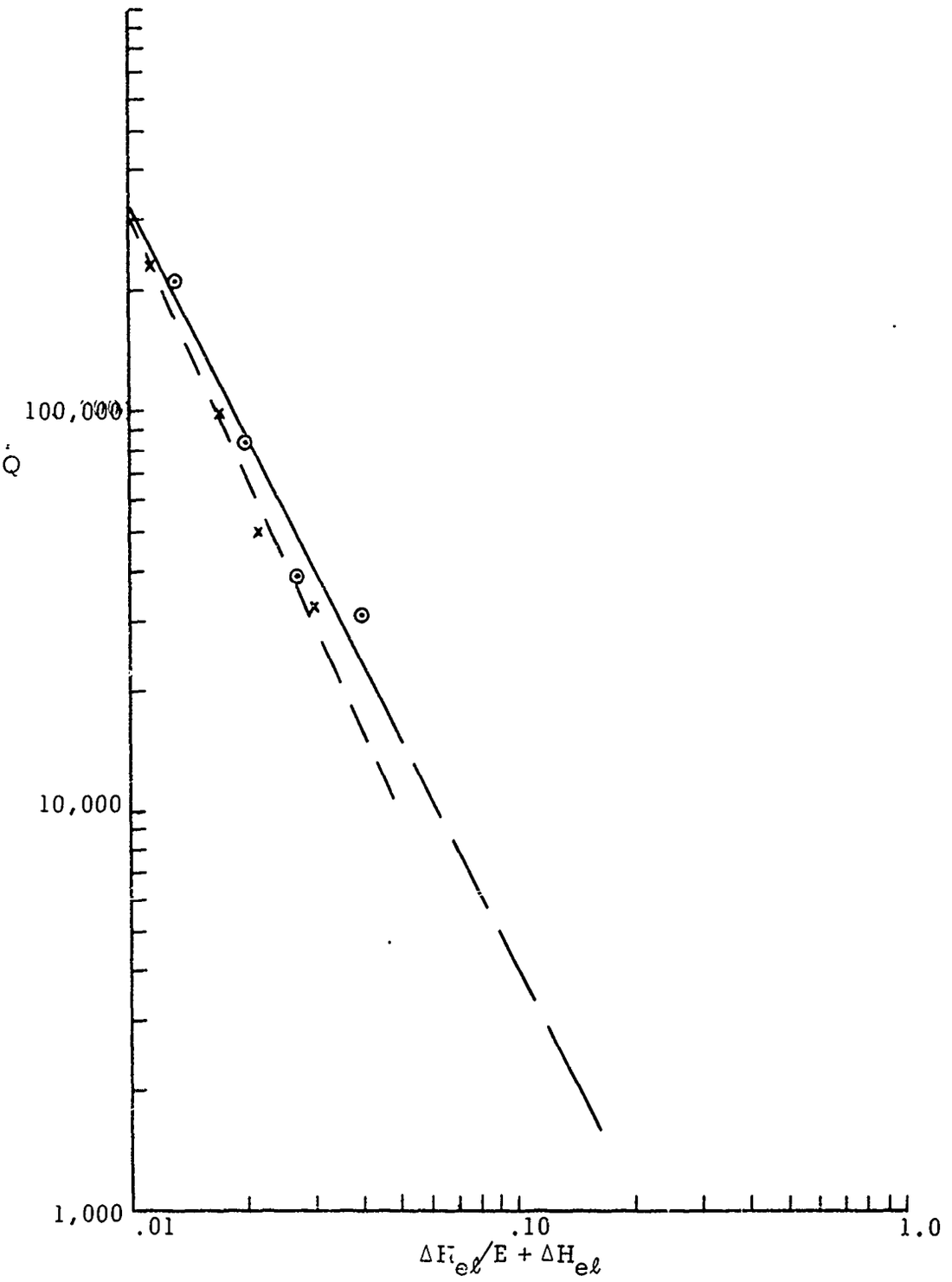

Figure 21. Decrease of $\dot{Q}$ with Increase of $\Delta H_{e\ell}/E + \Delta H_{e\ell}$ or $\Delta H_{e\ell}/E$

2.0 HYDRAZINE MONOPROPELLANT ENGINE

a. Engine Design

Based on the principle of electrolytic ignition of hydrazine, two monopropellant engines have been designed and fabricated. The first design, as shown in Figure 22, consisted of a lucite plate 3 1/2" x 2 3/4" x 3/8". An electrode cavity, 1 1/2" long, 30" wide was being fabricated along the middle of the plate. One end of the electrode cavity led into an expansion chamber .75" by .70" with an exhaust nozzle of .09" diameter. Hydrazine was introduced through the other end of the electrode cavity. The electrodes consisted of two stainless steel screens 1 1/2" x 3/4" separated from each other by a porous mica insulator. The screens and the mica insulator were fitted into the electrode cavity. Two specially fabricated stainless steel screws were used to make good electric contact with the screens so that desired voltage drop across the electrodes could be achieved. Two lucite windows, 3 1/2" x 2 3/4" x 1/4" were used to cover the entire configuration.

A photograph of the second design is shown in Figure 23. The electrodes consisted of two 1 1/2" long concentric cylinders with 0.368 inch I.D. and 0.348 inch O.D. respectively. The electrode gap space was thus 0.010 inch. A Kel-F gasket was used to insulate the electrodes from each other. The outer electrode also served as the chamber wall. Hydrazine was introduced to flow between the concentric electrodes and a 0.038 inch nozzle was used and pressure transients were recorded using a taper transducer.

b. Flow System and Recording Equipment

A schematic of the hydrazine flow system is shown in Figure 24. The flow systems were fabricated with 304 stainless steel lines. The propellant tanks were designed for a work pressure of 1000 psia. The tank capacities were approximately 1/3 gallon. Pressurization of the tank was controlled by a Grove regulator and a release valve which was set at 1000 psia. Two solenoid valves were used to vary the down pressure of the regulator. Propellant flow rates were controlled by the propellant tank pressure and also by variable area cavitating venturies. The flow controllers were micrometer head type. This device provided easy and precise control of the propellant flows. Propellant tanks and all the propellant supply lines from the tank to the injector were provided with heat exchangers. Propellant temperature was controlled by flowing coolant at the desired temperature through the heat exchangers. Prior to each test, the propellants were first led into a bypass tank until the desired propellant velocity and temperature were achieved before being introduced into the monopropellant engine.

Hydrazine flow rates were measured with a Cox turbine type flow meter. The flow meter output signals were fed into an amplifier to the oscillograph. The flow rate was determined from the meter frequency output and the propellant density. The applied current to initiate electrolytic ignition was determined by measuring potential drop across a specially designed 0.1 ohm precision resistor. Propellant temperatures at various locations were measured with I/C thermocouples, and a Taper transducer was used to record the engine chamber pressure. The entire experiment was operated remotely from a test control console which housed the propellant console panel, a test sequence unit, amplifier, and recording oscillograph with related

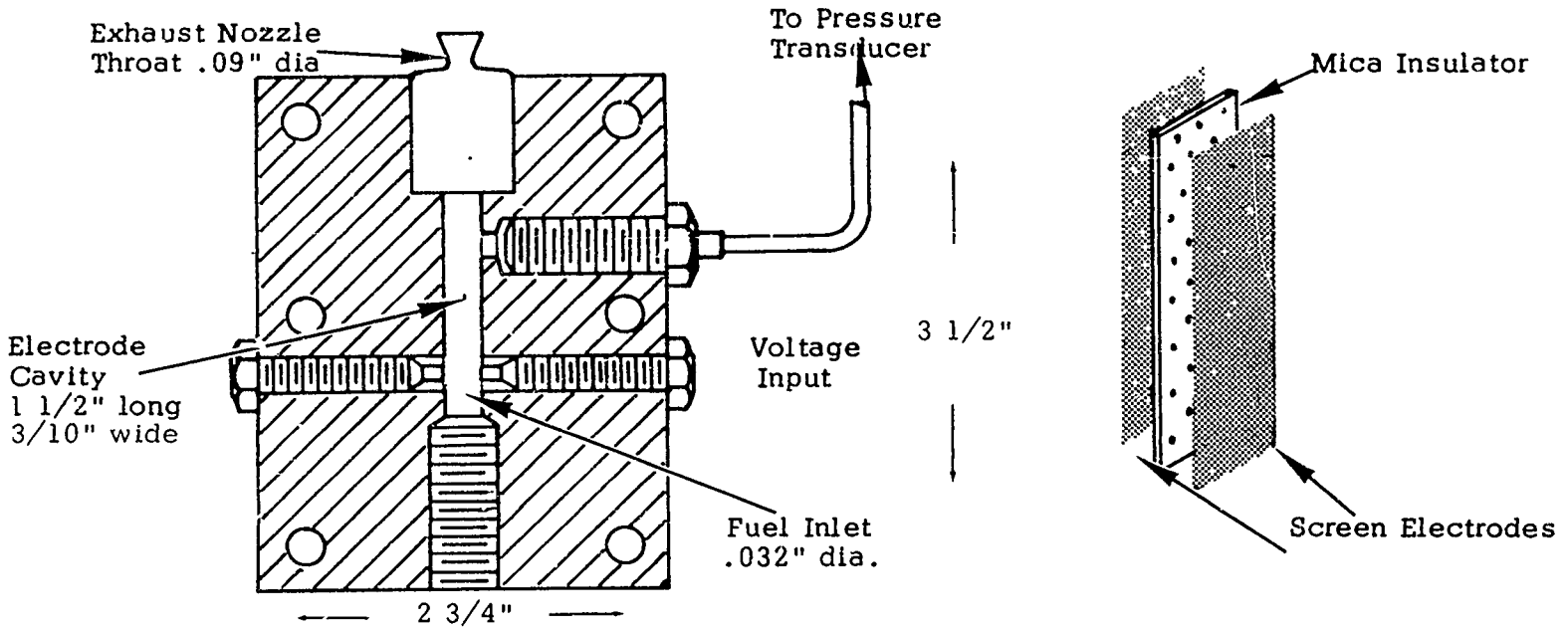

Figure 22. Transparent Monopropellant Engine.

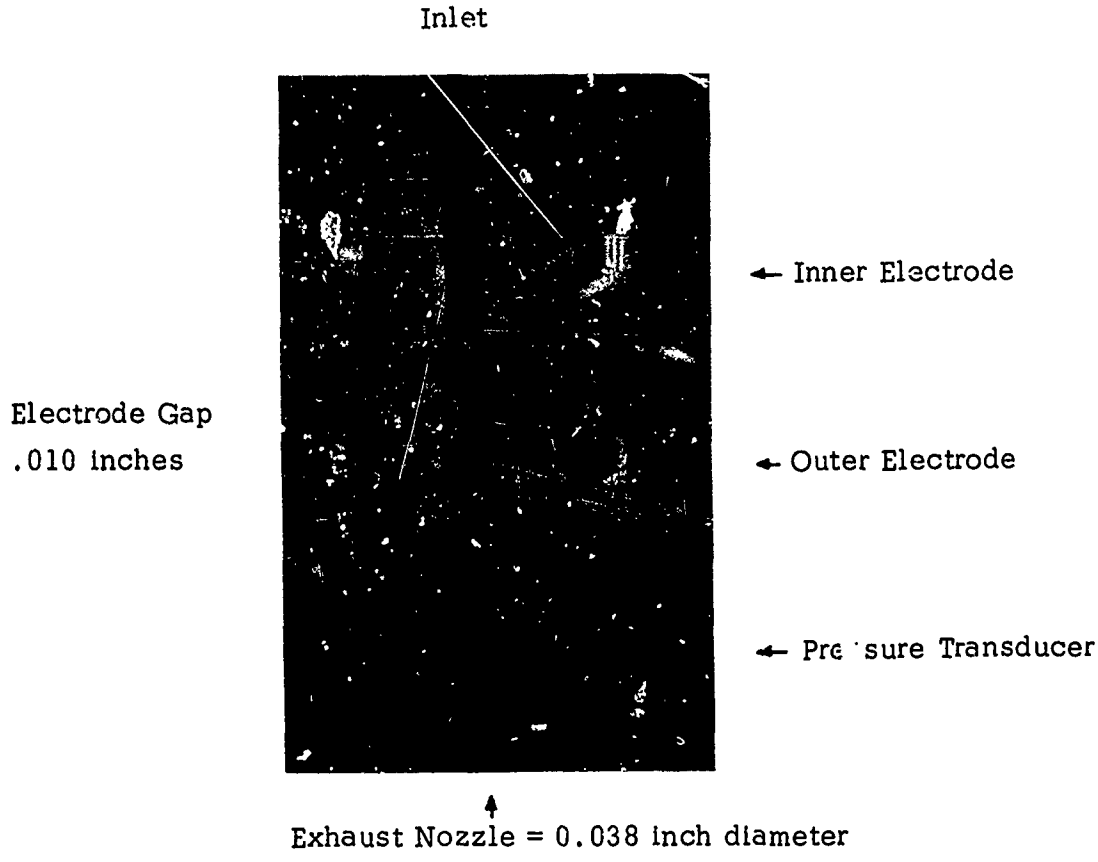

Figure 23. Stainless Steel Flow System - Concentric Configuration.

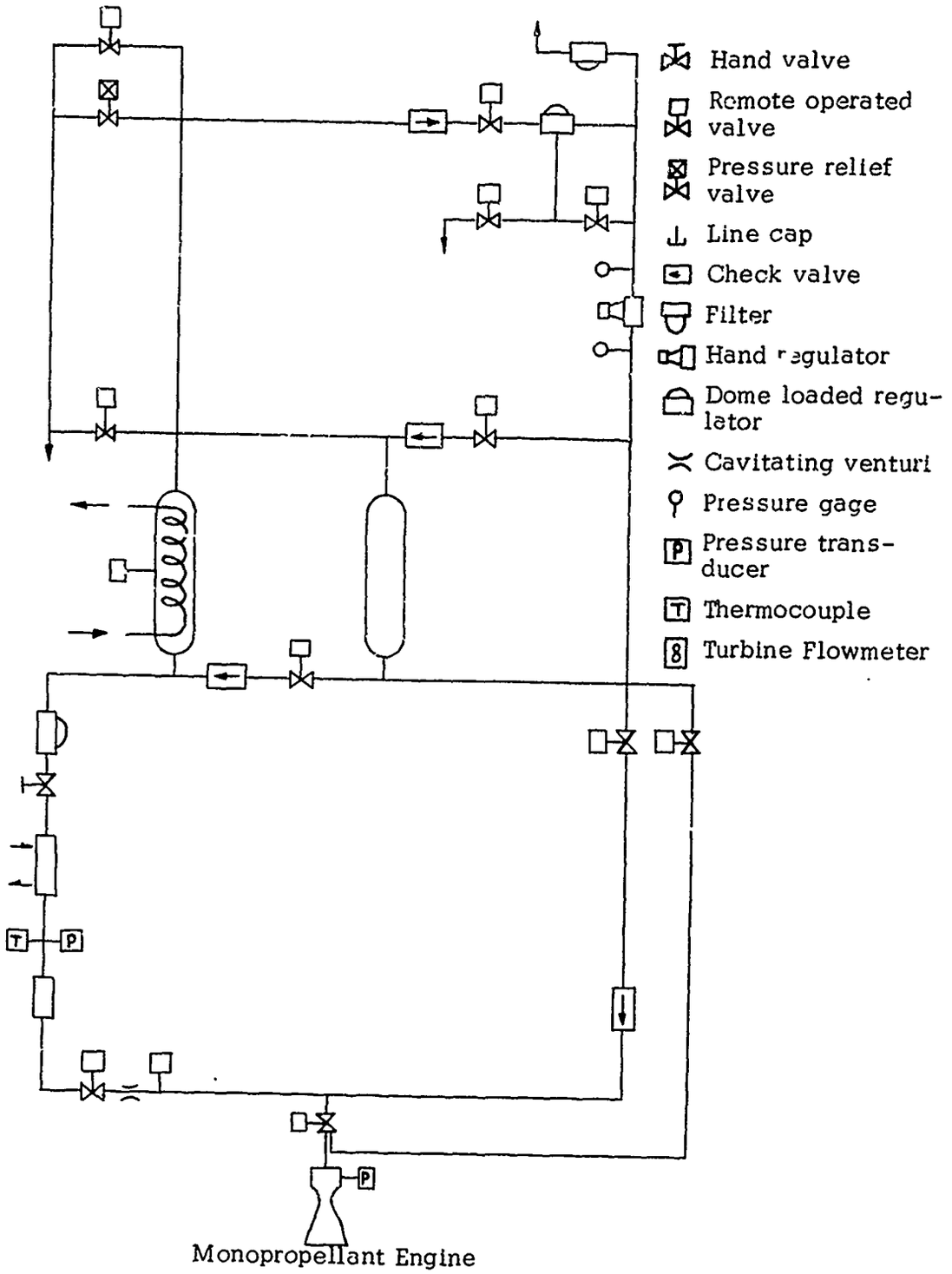

Figure 24. Hydrazine Flow System

components. The instrumentation system was centered around a Midwestern 801 recording oscillograph. Propellant flow rate, chamber pressure, current on-off signals and current amperage were recorded on the oscillograph. Propellant tank pressure was recorded on a strip recorder. Propellant temperatures at the flow meter and propellant tanks were recorded on a multipoint recorder.

c. Test Results

Successful engine starts were accomplished using the transparent lucite monopropellant engine as shown in Fig. 22. The reaction of the electrode cavity walls was a major problem, and meaningful test data were difficult to obtain. In order to remedy this problem the engine was modified by inserting the electrode screens and the porous mica insulator within a Pyrex sleeve 3/8" in diameter. Ignition is difficult to achieve because most of the propellant flowed through the spacing between the screens and the Pyrex sleeve instead of through the mica insulator.

An aluminum engine, identical to the lucite design of Figure 22 was also fabricated. Ceramic liners were used along the cavity wall to insulate the screen electrode from the aluminum plate. Engine ignitions were observed at flow rates of 2 cc/sec. with a 40 psi fuel tank pressure. Chamber pressures of approximately 20 psi were recorded. With proper thermal insulation and better controlled propellant injection systems reproducible and fast ignition transients can be obtained.

It was desirable to investigate the possibility of fabricating an all metal engine so that reliability and engine long life could ultimately be achieved. This results in the ultimate design of two concentric stainless steel cylinder electrodes. Numerous engine tests were conducted based on this model. Fast electrolytic ignition could often have been successfully accomplished, but often engine instability appeared to be a problem. This is to be anticipated since the purpose of these tests were designed to demonstrate the feasibility of electrolytic ignition and little consideration was devoted to the engine design for stable engine operation. One of the most promising and encouraging features of these tests was not only electrolytic engine start is feasible but ignition transient, t_{90}, is ofter within 5 ms after the current is applied. Figure 25 is a reproduction of the actual chamber pressure transient. The test was conducted with both propellant and engine temperature initially at $60^{\circ}F$. Propellant flow rate was .0022 lb/sec. The measured t_{90} was approximately 1.5 ms (with an applied current of 0.4 amps). This clearly demonstrated one great advantage of electrolytic ignition as compared with catalytic systems, that faster transient response of an order of magnitude can be achieved.

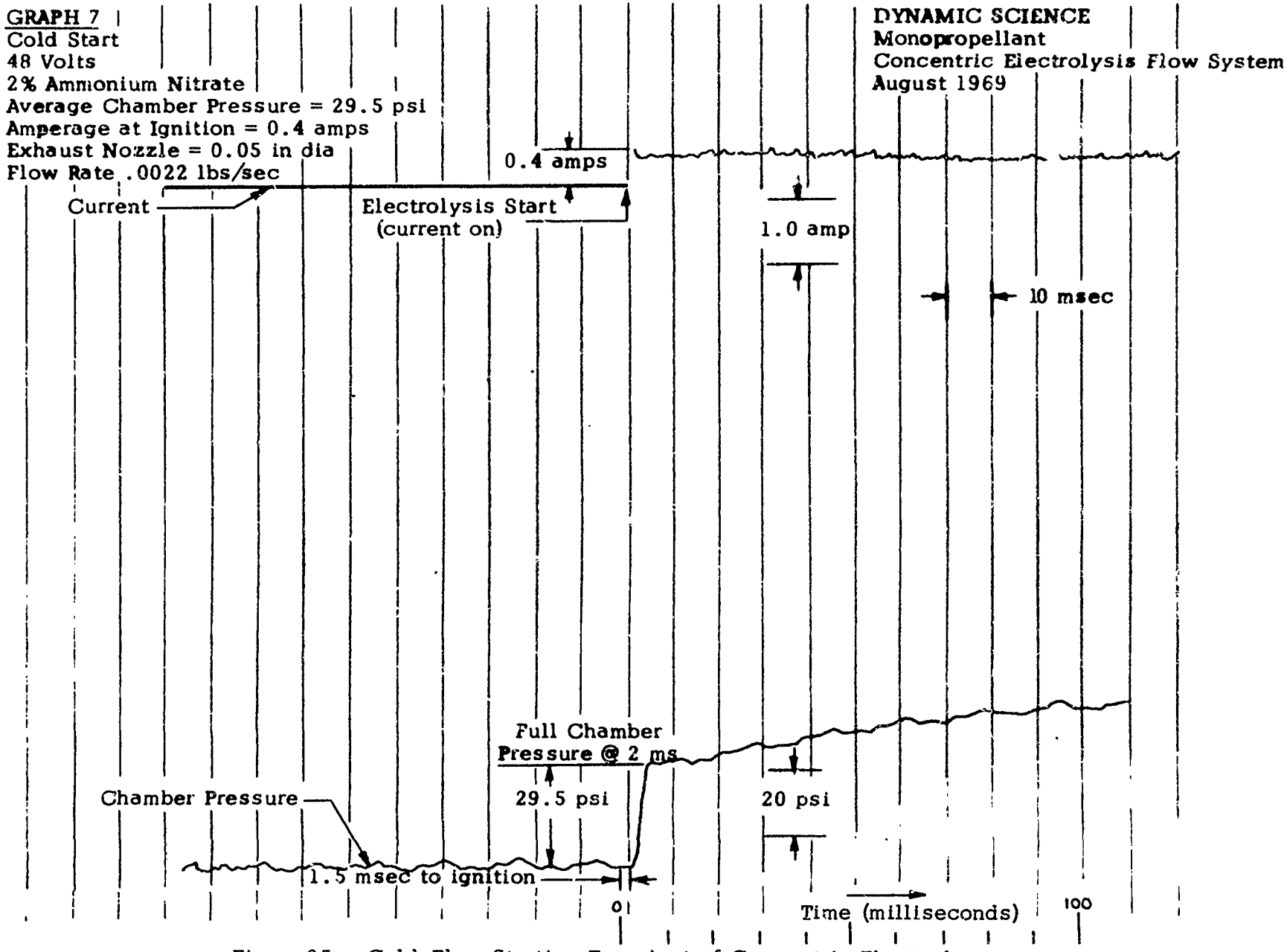

Figure 25. Cold-Flow Starting Transient of Concentric Electrode.

d. Conclusions

Based on these test results, it has been demonstrated that electrolytic ignition of a monopropellant engine is not only feasible but fast transient response can also be obtained. Using the electrolytic ignition device, many of the problem areas associated with the catalytic system are simultaneously removed; such as physical loss of catalyst; loss of catalytic activity; sintering and clogging of injectors with catalytic fines and the problem associated with the nonavailability of catalytic materials. With an all metal engine design, better engine reliability and longer engine life can be attained. Reproducible pulses can be obtained since electrolytic ignition is less temperature dependent and with faster ignition response resulting in better pulse shape. The electrolytic monopropellant engine has the potential of achieving better performance, capable of handling a variety of propellant blends and for propellant grade hydrazine the engine can be easily designed to yield lower NH_3 dissociation.

SECTION IV

CONCLUSIONS AND RECOMMENDATIONS

The ability to produce rapid electrolytic ignition in a simulated 1/2 thrust configuration has been demonstrated. The results show that an electrolytic ignition system does represent a practical approach to monopropellant, pulsed thrusters.

The problems encountered during this effort appear to involve vapor generation and electrical insulation of the electrodes. It is felt that these problems can easily be overcome by proper injector flow distribution and electrothermal design. Vapor formation at an electrode is commonplace in electrochemistry. In this application, the vapor generation is the heat source and thus, by enlarging the electrode area again with screens or microscopically porous material, the vapor and heat generation may be maximized while heat loss is minimized.

It was beyond the scope of the present effort, however, to optimize the system, although the variables necessary to optimize ignition delay were investigated. It is recommended that subsequent effort should involve optimization of the combined flow and electrical system. Such a program would provide the basis or prototype for manufacture of flight weight hardware and would involve testing of the complete thrustor performance during pulse and steady-state operation as compared with the work reported here which emphasized engine start-up.

SECTION V

REFERENCES

1. Ferguson, Harold and Sovey, J. S., "Performance Tests of a 1/2 Millipound (2.2 mN)Ammonia Resistojet Thrustor System," NASA TN D-4249, November 1967.

2. John, Richard R., "Resistojet Research and Development Phase II, Design Development and Fabrication of an Ammonia-Fueled Resistojet Thrustor System," Final Report, prepared for NASA Contract NAS3-5908, December 1966.

3. Schreib, R. R., Rugmire, T. K., and Chopin, S. G., "The Hybrid (Hydrazine) Resistojet," Paper No. 69-496 AIAA 5th Propulsion Joint Specialist Conference, June 1969.

4. Butcher, W. W., Lodwig, R. M., Jones, W. H., and Morgan, N. E. "Hydrazine Electrolysis for Spacecraft Propulsion," Final Report/JPL Contract No. 951720/August 1968/SSD 80316R, Hughes Aircraft Co., Space Systems Division.

5. Eckert, E. P. G. & Drake, R. M. "Heat and Mass Transfer," McGraw-Hill Book Co., New York (1959), pp 175 & pp 140.

6. Jost, Wilhelm, Explosion and Combustion Processes in Gases, McGraw-Hill Publications in Aeronautical Science, New York, 1946.

Unclassified

Security Classification

DOCUMENT CONTROL DATA - R & D

(Security classification of title, body of abstract and indexing annotation must be entered when the overall report is classified)

1 ORIGINATING ACTIVITY (Corporate author)	2a. REPORT SECURITY CLASSIFICATION
Dynamic Science, a Division of Marshall Industries 2400 Michelson Drive Irvina, California 92664	Unclassified
	2b. GROUP

3 REPORT TITLE

ELECTROLYTIC IGNITION SYSTEM FOR MONOPROPELLANTS

4. DESCRIPTIVE NOTES (Type of report and inclusive dates)

Final Report - January 31, 1969 - October 31, 1969

5. AUTHOR(S) (First name, middle initial, last name)

B. P. Breen, M. Gerstein, and M. A. McLain

6. REPORT DATE	7a. TOTAL NO. OF PAGES	7b. NO. OF REFS
January 11, 1970	64	5

8a. CONTRACT OR GRANT NO.	9a. ORIGINATOR'S REPORT NUMBER(S)
F04611-69-C-0048	SN-147-F
b. PROJECT NO	
c.	9b. OTHER REPORT NO(S) (Any other numbers that may be assigned this report)
d.	AFRPL-TR-69-247

10 DISTRIBUTION STATEMENT

This document is subject to special export controls and each transmittal to foreign nationals may be made only with prior approval of AFRPL(RPOR/STINFO), Edwards, California 93523

11. SUPPLEMENTARY NOTES	12. SPONSORING MILITARY ACTIVITY
	Air Force Rocket Propulsion Laboratory Air Force Systems Command Edwards, California

13 ABSTRACT

It was the objective of this work to utilize the electrolytic decomposition of hydrazine toward the improvement of starting pressurization transients in monopropellant rockets. The electrochemistry and heat generation involved during the electrolytic decomposition of propellant grade hydrazine was examined by means of polarography and chromatographic examination of the decomposition gases. Critical voltages of decomposition and related data obtained were incorporated into a thermal ignition model to aid in the design of a flow system ignition cell.

It was found that engine ignition times of 2 to 5 milliseconds and pulse start transients of less than 15 milliseconds could be obtained in a simulated one-half thrust configuration. The ignition data and chamber pressure traces included in this report demonstrate the reproducibility of electrolytic ignitions through the electrolytic decomposition of hydrazine. Although the primary concern of this work was engine start-up, variables necessary to optimize ignition delay and maintain sustained engine operation after start-up were investigated. Total optimization of the system was beyond the scope of this present effort.

DD FORM 1 NOV 65 1473

Unclassified

Security Classification

14. KEY WORDS	LINK A		LINK B		LINK C	
	ROLE	WT	ROLE	WT	ROLE	WT
Hydrazine						
Electrolysis						
Monopropellant Ignition						
Monopropellant						
Ignition						